



# The tholeiites of the Valaisan domain (Versoyen, western Alps): a Carboniferous magma emplaced in a small oceanic basin

Jean-Louis Mugnier, S. Cannic, Henriette Lapierre

## ► To cite this version:

Jean-Louis Mugnier, S. Cannic, Henriette Lapierre. The tholeiites of the Valaisan domain (Versoyen, western Alps): a Carboniferous magma emplaced in a small oceanic basin. Bulletin de la Société Géologique de France, 2008, 179 (4), pp.357 à 368. 10.2113/gssgfbull.179.4.357 . insu-00351987

**HAL Id: insu-00351987**

**<https://hal-insu.archives-ouvertes.fr/insu-00351987>**

Submitted on 12 Jan 2009

**HAL** is a multi-disciplinary open access archive for the deposit and dissemination of scientific research documents, whether they are published or not. The documents may come from teaching and research institutions in France or abroad, or from public or private research centers.

L'archive ouverte pluridisciplinaire **HAL**, est destinée au dépôt et à la diffusion de documents scientifiques de niveau recherche, publiés ou non, émanant des établissements d'enseignement et de recherche français ou étrangers, des laboratoires publics ou privés.

**Les tholéïtes du domaine Valaisan (Complexe du Versoyen, Alpes occidentales):**

**un magma carbonifère dans un petit bassin océanique**

**The tholeiites of the Valaisan domain (Versoyen, western Alps): a Carboniferous magma  
emplaced in a small oceanic basin**

Jean-Louis Mugnier , Sebastien Cannic, and Henriette Lapierre

LGCA, UMR 5025 CNRS et Université de Savoie, Batiment les Belledonnes, 73376, Le Bourget du  
lac Cedex, France. Correspondance: [jean.louis.mugnier@univ-savoie.fr](mailto:jean.louis.mugnier@univ-savoie.fr)

**Key words:** Alps, geodynamics, structural inversion, suture

**Abstract**

The mafic-ultramafic assemblages of the Versoyen complex exposed in the Valaisan domain is close to the boundary between the Internal and the External domains of the Western Alps. Zircons extracted from the Versoyen complex suggest an emplacement during Paleozoic times, and probably during the Viséan (~337 Ma). The base of the Versoyen complex is formed of laccoliths and sills associated with black shales, while pillow basalts and tuffs predominate at the uppermost levels. Locally, basaltic dikelets intruded leucocratic gneiss. Ultramafic-mafic cumulates form the bottom of the thickest intrusions while diabases are present along the chilled margins. All these rocks have been affected by a polyphased metamorphism under eclogitic to blueschist and greenschist facies conditions. Magmatic textures have been destroyed and the igneous mineralogy is seldom preserved. The mafic rocks of the Versoyen complex show tholeiitic to alkali-transitional affinities. The pillow basalts and the sill cores have flat REE patterns characteristic of N-MORB and T-MORB. Their  $\epsilon_{\text{Nd}}$  (assuming an age of 337 Ma) ratios range from +5.7 to +9 which suggest a mixing of N-MORB and OIB sources. The sill margins show Th, U and LREE-enrichments and negative  $\epsilon_{\text{Nd}}$  ratios. These features are likely related to contamination when hot mafic magmas intruded unconsolidated sediments rich in water. The high Th, U, LREE abundances and low  $\epsilon_{\text{Nd}}$  ratio of the basaltic dikelet are probably related to crustal contamination occurring during the magma ascent. The geochemical characteristics of the Versoyen rocks are compatible with a tholeiitic magma emplaced into a small oceanic basin in the vicinity of a continent. The importance of the pre-Mesozoic crustal thinning evidenced in one segment of the

boundary between the Internal and External zones of the Alps suggests that the Pennine Front is an Alpine mega-thrust inherited from a Variscan suture.

**Mots clés:** Alpes, géodynamique, inversion structurale, suture

## Résumé

Le complexe de roches mafiques du Versoyen est situé à la limite entre les zones externes et internes des Alpes occidentales. Un âge Paléozoïque [Cannic, 1996], probablement Viséen [Masson et al., ce volume] est suggéré par des datations de Zircons provenant de ce complexe. La base du Versoyen est formée de laccolites et de sills associés avec des schistes noirs, tandis que les pillow-lavas et les tufs dominent dans la partie supérieure. Localement, à la base, des gneiss leucocrates sont pénétrés par des petits dykes basaltiques. Des cumulus ultrabasiques forment la base des plus grosses intrusions et des diabases sont situées aux éponges. Toutes ces roches sont affectées par un métamorphisme polyphasé, depuis des conditions éclogitiques jusqu'à des conditions schistes vert. La plupart des textures magmatiques ont été détruites, et la minéralogie initiale est rarement préservée. Le Versoyen montre des affinités des roches mafiques de type tholéitique à alcalin-transitionnel. Les pillow-lavas et le centre des sills montrent des diagrammes REE plats, caractéristiques de N-MORB ou de T-MORB. Leur rapport  $\epsilon_{Nd}$  (en supposant un âge de 337 Ma) est situé entre +5.7 et +9, ce qui suggère un mélange de sources composé de N-MORB et d'OIB. Les éponges des sills montrent des enrichissements en Th, U et LREE et des rapports  $\epsilon_{Nd}$  négatifs. Ceci est probablement lié à une contamination lors de la pénétration du magma chaud dans les sédiments riches en eau et non consolidés. L'abondance en Th, U et LREE ainsi que la faible valeur du rapport  $\epsilon_{Nd}$  des petits dykes basaltiques est probablement liée à une contamination crustale durant l'ascension du magma. Les caractéristiques géochimiques du Versoyen sont compatibles avec celles d'un magma mis en place dans un petit bassin océanique, à proximité d'un continent. L'importance de l'extension pré-Mésozoïque mise en évidence par le Versoyen à la limite entre Alpes externes et Internes suggèrent que le front Pennique est un chevauchement majeur hérité d'une suture varisque.

## INTRODUCTION

The Alps are classically presented as the product of convergence and collision between Eurasia and Africa plates. In the most classical model [Pavoni, 1961; Steck, 1990], the Alps were formed during the (1) N-S to NW-SE trend convergence between Europe and Apulia, (2) closure of an oceanic domain followed by an eastward subduction and (3) collision between Eurasia and Africa. The oceanic suture is nowadays exposed along the Piemonte-Ligurian domain in the Chenaillet and Monviso massifs and the Zermatt-Saas zone [Lemoine, 1980; Bertrand et al., 1982; Colombi & Pfeifer, 1986; Lagabrielle, 1987]. However ultramafic-mafic igneous rocks are not restricted to the Piemonte-Ligurian domain, but are also exposed in the lower Penninic units of the western Alps. Therefore, a complex Mesozoic oceanic pattern, involving at least a Piemonte and a Valaisan ocean is frequently inferred [Frisch, 1979; Stampfli, 1993; Rosembaum and Lister, 2005].

The Versoyen Complex, located in the vicinity of the Mont-Blanc massif (Fig. 1), represents the greatest ultramafic-mafic assemblage of the lower Penninic units. Different interpretations have been proposed for the genesis of the Versoyen Complex. For Loubat [1968] and Antoine [1971], the Versoyen Complex represents an ophiolitic suite developed in a basin floored by oceanic crust. In that case, the Versoyen Complex is considered as a klippe of Piemonte-Ligurian domain [Schoeler, 1929; Bocquet 1974] or a part of an oceanic Valaisan domain distinct from the Piemonte-Ligurian domain [Antoine, 1971; Stampfli, 1993]. However, the magmatic affinity of the meta-igneous rocks is poorly defined and their sources are not characterized.

Thus, the distribution and the composition of the igneous and sedimentary rocks of the Versoyen Complex as well as its age and the chemistry of the igneous component are salient for testing the various interpretations and for the understanding of the geodynamic evolution of the western Alps.

This paper focuses on petrology, trace element and Nd-Sr isotopic geochemistry studies of the Versoyen igneous rocks. The studied areas are located near the Petit Saint Bernard pass (PSB, Fig. 1) along the border between France and Italy and near Visp (Switzerland). These new data allow us to determine the geologic significance of the Versoyen Complex and to reconsider the paleogeography of the European margin and its geodynamical evolution during the Alpine history.

## **GEOLOGICAL SETTING**

The axial zone of the Alpine belt is classically divided into external and internal zones following the paleogeographic setting of the rocks. The Valaisan domain represents the north-western part of the internal zone. This domain is composed of (i) the Valaisan flysch (or "flysch de Tarentaise" of Antoine [1971]), (ii) the igneous and sedimentary pile of the Versoyen Complex, (iii) the substratum of the Moutier unit, and (iiii) the metapelites of the Petit Saint Bernard (PSB) unit.

### **Structure the Versoyen Complex**

The southern termination of the Valaisan domain near the PSB pass is bounded to the E and to the W by two major thrusts which are respectively the Briançonnais Front (BF) and the Penninic Thrust (PT) (Fig. 2). The Valaisan domain is constituted of imbricated thrust sheets [Barbier, 1951; Trumphy, 1955; Butler, 1984]. The Versoyen Complex is bounded to the East by the Petit Saint Bernard unit and to the West by the Valaisan flysch and is composed by a 400-500 m thick pile of sediments, mafic and ultramafic rocks. The metamorphic history of the Versoyen Complex is polyphased. The Alpine orogeny is responsible for the eclogitic event and the retromorphic stages under blueschist and greenschist facies conditions [Schurch, 1987; Cannic et al., 1996, Bousquet et al., 2002]. During the magmatic cooling, the rocks were affected by an alteration due to water circulation (spilitisation of Lasserre and Laverne, 1976].

Near Visp (Switzerland), a meta-igneous complex of the Valaisan domain has some facies affinity with the Versoyen Complex and is highly deformed. It consists of mafic layers and ultramafic rocks [Dietrich and Oberhansli, 1975] located in a less than 200 m thick sedimentary pile (Fig. 3). It is tectonically associated with the Visperterminen serie ("Zone Houillere") and is clearly distinct from the Jurassic volcanics series of the "Pizzo del Vallone Nappe" [Carrupt 2003]. It is affected by a sub-horizontal axial plane cleavage fold pattern [Jeanbourquin, 1994]. The major metamorphic event seems epizonal to mesozonal [Colombi, 1989; Jeanbourquin and Burri, 1991].

The age of the Valaisan domain remains uncertain. The Valaisan flysch is assumed to be Senonian to Campanian [Antoine, 1971] or Priabonian [Gely, 1989] in age. For Antoine [1971], the calcareous slates of the Petit Saint Bernard would represent the basement of the Versoyen Complex which in turn

would represent the base of the Valaisan flysch and a relative age would be deduced for the different units. However, this assumption is highly questionable because the Petit Saint Bernard unit thrusts above the Versoyen Complex [Fudral, 1973; Lasserre and Laverne, 1976] and the Versoyen above the Valaisan flysch [Mugnier et al., 1993; Goffe et Bousquet, 1997; Masson, 2002].

### **Lithostratigraphic sequence of the Versoyen Complex**

The Versoyen Complex is presently formed by isoclinal folds with successively (at least 5 times) normal and overturned beds [Cannic et al., 1996]. Furthermore, a décollement occurred along serpentinized ultramafic levels and keeps difficult the restoration of the lithostratigraphic sequence. We assume that the lower levels of the Versoyen Complex are the gneiss and leptynites relics of the "Pointe Rousse" [Loubat, 1968] near the PSB pass (Fig. 3). The major part of the sequence consists of a succession of mafic sills and/or laccoliths interbedded with sediments. These sediments are composed of black shales, arkoses or greywackes [Antoine 1971]. The upper part of the lithostratigraphic succession is composed of pillow basalts, pillow breccias, mafic tuffs and black shales.

The thickness of the sills and/or laccoliths ranges from 0.5 to 40 m. Cumulate gabbros or ultramafic rocks are located at the base of the thickest sills, just above the lower chilled margin. The uppermost part of the sills is composed of dolerite located immediately beneath the upper chilled margin. The mafic sills are locally intruded by small felsic dikes which do not show chilled margin. This suggests that the felsic dikes intruded within still hot igneous rocks. A metamorphic basement, composed of leucocratic gneiss and leptynite, is located along the SE boundary of the Versoyen Complex. These metamorphic rocks are intruded by 0.1 to 5m broad basaltic dikelets. These dikelets could either be the early products of the Versoyen igneous activity in a basin still floored by continental crust or be contemporaneous with the other rocks of the Versoyen Complex but emplaced along the continental margins of the basin [Cannic, 1996].

Near Visp, the lithostratigraphic sequence shows similar lithologies. However, the serpentinized ultramafic bodies are more developed and are intruded by gabbroic rocks. The black shales are associated with calcareo-dolomitic breccias, conglomerates and siliceous pelagic limestones.

## **The age of the Versoyen Complex**

The Versoyen Complex was assumed to be of Late Jurassic-Early Cretaceous age [Antoine, 1971]. However, this age is clearly a matter of debate, because the sediments associated with the igneous rocks never yielded paleontologic relics. Furthermore, there is no evidence that the limestone blocks found in a sill of the Versoyen Complex are Jurassic in age, as postulated by Loubat [1968] or Antoine et al. [1973].

Four fractions of zircon have been separated from a cross-cutting leucogabbro dyke by Cannic [1996] and the main gabbroic body intruded into the Versoyen series has been sampled at three places by Bussy et al. [2005]. The zircons have been analysed by the U-Pb method, defining a regression line that intercepts the Concordia curve. A lower zircon intercept at 294 Ma has been obtained by Cannic [1996]. An alternative Pb corrections defines a lower intercept age at  $309 \pm 6$  (2  $\sigma$ ) Ma and an upper intercept age at  $3240 \pm 34$  Ma [Schärer et al., 2000]. These intercepts respectively date the emplacement of the leucogabbro into the Versoyen Complex, and the age of inherited Archean zircon cores, located in the newly formed crystals [Schärer et al., 2000]. Three samples of the main gabbroic body analysed by Bussy et al., [2005] and Masson et al., [this volume] furnish well grouped analytical data very near the Concordia curve and give a crystallization age of  $337 \pm 4.1$  Ma [].

The chronological dating therefore characterises a carboniferous age for the Versoyen Complex [Cannic, 1996; Schärer et al., 2000; Bussy et al., 2005; Masson et al., in press ].

## **PETROLOGY OF THE VERSOYEN IGNEOUS ROCKS**

The hydrothermal alteration and the Alpine metamorphism have destroyed the igneous textures. The primary igneous mineralogy is replaced by the metamorphic paragenesis. The most common assemblage is albite  $\pm$  clinozoisite  $\pm$  actinolite  $\pm$  chlorite  $\pm$  sphene  $\pm$  phengite  $\pm$  ilmenite  $\pm$  quartz [Loubat 1968]. However, doleritic to cumulate textures and augitic pyroxene are preserved in the less metamorphosed rocks.

- The cumulate metagabbros show heteradcumulate (92-18, Va-5, Va- 11 on Fig. 3) to mesocumulate (92-19, 92-35, Va-12) textures. The plagioclase is surrounded by euhedral to anhedral



clinopyroxene generally altered to omphacite, actinolite and/or chlorite. The clinopyroxene exhibits augite to Mg-rich diopside compositions (Table 1 and Fig. 4a). Clinopyroxene compositions are indicative of the magmatic affinity of the rocks in which they occur [Nisbet and Pearce, 1977; Leterrier et al., 1982]. In a Ti+Cr versus Ca plot [Leterrier et al., 1982], all the clinopyroxenes fall in the anorogenic field (Fig. 4b). They show homogeneous Ca content but their Ti+Cr contents are variable. In a Ti versus Al<sub>total</sub> plot (Fig. 4c), they cluster in the tholeiitic field.

- The dolerites occur as sill margins (93-16, 92-06, 91-12, 92-16, 92-21) and pillow basalts (92-10, 92-22, 92-24, 92-42). They are characterized by doleritic to intersertal textures and an important variation in the grain size. They consist of plagioclase laths pseudomorphosed in albite. The other primary mineralogy is completely replaced by the metamorphic paragenesis.

- The aphyric basalts occur as dikelets (93-03, 94-62) intruding the gneiss. They are characterized by albite microlites and a groundmass completely replaced by chlorite.

- The felsic rock (94-104) is characterized by euhedral plagioclase laths now replaced by albite. The patches between the plagioclases are filled with chlorite, actinolite and quartz. This felsic rock includes igneous zircons [Scharer et al., 2000] and thus is Zr-enriched (see Table 2).

- In the less deformed ultramafic rocks, olivine and Cr-rich spinel appear to be cumulus phases while pyroxene is intercumulus. Olivine and orthopyroxene are generally replaced by antigorite and chrysotile ± talc respectively. Clinopyroxene is rarely preserved. Most frequently, it is altered to blue Na-rich amphibole which is in turn replaced by green hornblende or even actinolite. The serpentinized ultramafic bodies were interpreted as the remnants of depleted mantle by Loubat and Delaloye [1984]. However, the only preserved textures are cumulate would indicate that the serpentinites are altered cumulate ultramafic rocks located within the thickest intrusions.

In the Visp area, serpentinites show mylonitic microstructure with chrysotile ± talc tabular porphyroblasts in a serpentinized groundmass. These serpentinites could represent altered layered peridotite. The crystallization sequence observed in the mafic rocks is:

olivine ---> plagioclase ---> clinopyroxene ---> Ti-Fe oxide.

## **GEOCHEMISTRY OF THE META-IGNEOUS ROCKS**

### **Sampling and analytical techniques:**

The composition of the Versoyen mafic rocks was investigated by analyzing 22 rocks, and clinopyroxenes were separated from a cumulate gabbroic sill core (95-23).

Rock powder samples were prepared using agate mortars in order to avoid any contamination.

Major and minor elements were analyzed by G. Mevelle at the Centre de Recherche Pétrographique et Géochimique (CRPG) of Nancy. Relative standard deviations are less than 2 %.

Trace elements and Rare Earth Elements (REE) were analyzed by ICP-MS using two different techniques: acid dissolution and fusion with Lithium borates. The samples were measured at the Laboratoire of the Department of Geology, Musée de l'Afrique Centrale, Tervuren, Belgique, with analytical errors of 1.5 to 3 % and at the Laboratoire de Géochimie de l'Université Paul Sabatier, Toulouse, France.

Before dissolution, the separated clinopyroxenes were cleaned up with HCl (2N) and washed using Mi11Q™ water (leaching method). Dissolution of 100 mg of sample was carried out with HF (22.6N) + double-distilled HN03 (13N) + HC104 (11.6N) mixture. This mixture was heated at 100°C during 2 hours. After cooling, the solution was evaporated to dryness. The residue was dissolved with double-distilled HN03.

For the fusion with Lithium borates, 100 mg of powdered rock are weighted in a Pt crucible with 320 mg of Lithium metaborate and 80 mg of Lithium tetraborate (Fluka). After careful mixing of the powders, the crucible is heated for fusion at 1000°C. After cooling, 8 ml double-distilled HN03 and HF are added for the dissolution of the glass.

The final dilution to 30 ml aliquot, with Mi11Q™ water and after addition of internal standards (In-Re) corresponds to a total dilution of 3000. The precision of the technique is better than 10  $\sigma$  for compatible elements (Cr, V, Ni) and 3  $\sigma$  for all the REE and incompatible elements.

Nd and Sr isotopic compositions were determined on a Finnigan MAT261 multicollector mass spectrometer at the Laboratoire de Géochimie de l'Université Paul Sabatier in Toulouse.

Dissolution of ~100 mg samples was realized in closed teflon screw cap vessels with a HF-HClO<sub>4</sub> mixture and converted to chloride form using HCl. Chemical separation of Sr was carried out on a AG50W (200-400 mesh) cationic ion exchange column. NBS standard was measured with a <sup>87</sup>Sr/<sup>86</sup>Sr ratio of 0.71025 (mean of 200 ratios) corresponding to an external reproductibility of 0.00003.

Nd separation was carried out using two stages exchange reverse chromatography AG50WX8 cationic ion exchange column, followed by HDEHP orthophosphoric column. Results on La Jolla Nd standard yielded <sup>143</sup>Nd/<sup>144</sup>Nd = 0.511850 ± 8 (mean on 39 runs) corresponding to an external reproductibility of 0.00001.

The geochemical results (Major and trace elements) of the Versoyen Complex and the meta-igneous complex of Visp are respectively summarized in Table 2 and 3, whereas the Sr and Nd compositions are given in Table 4.

#### **Major element composition and effects of oceanic alteration and Alpine metamorphism in the chemistry of the Versoyen igneous rocks:**

Generally, hydrothermal alteration and metamorphism of the igneous rocks are mainly expressed by high Loss On Ignition (LOI). In most of the analyzed rocks, LOI ranges from 2 to 6 wt %. However, some rocks have very high values which range between 9 and 13 wt %. The high LOI contents of these rocks are likely related to the abundant chlorite of the groundmass. The highest values of LOI correlate with the lowest values of SiO<sub>2</sub>. This SiO<sub>2</sub>-depletion is easily explained by the mobility of silica in the altered samples. Thus, the polyphased metamorphism which has affected the Versoyen Complex precludes the use of major elements for the characterization of the affinities of the igneous rocks with the exception of TiO<sub>2</sub>, MgO and Fe<sub>2</sub>O<sub>3</sub>.

The Al<sub>2</sub>O<sub>3</sub>, Fe<sub>2</sub>O<sub>3</sub> and MgO values support the tholeiitic nature of the magmatism. However, TiO<sub>2</sub> content (> 1.42 wt %, Table 2) is rather high when compared to those of the tholeiitic rocks. The felsic rock shows a mafic composition (SiO<sub>2</sub> = 49 wt%) in spite of the presence of quartz. The high Al<sub>2</sub>O<sub>3</sub> value of this rock is supported by the Albite abundance. The TiO<sub>2</sub>, Fe<sub>2</sub>O<sub>3</sub> and MgO contents are similar to those of the gabbroic cores. The basaltic dikelets are SiO<sub>2</sub>- and TiO<sub>2</sub>-poor, MgO-, Al<sub>2</sub>O<sub>3</sub>- and Fe<sub>2</sub>O<sub>3</sub>-rich

### Trace element abundances:

The cores and margins of the tholeiitic sills, the pillows basalts and the felsic rock show low Ni - contents ( $\leq 166$  ppm) suggesting that rocks are not primitive mantle-derived melts. The basaltic dikelet shows high Ni ( $> 430$  ppm) and low Cr-V contents. The separate clinopyroxene shows trace element abundances (Table 1) similar to those of the gabbroic host rock with the exception of Nd and Ba.

The Ti/Y versus Nb/Y [Pearce 1982] diagrams using trace elements considered immobile during alteration and metamorphism processes, the samples cluster in the tholeiitic field with the exception of the basaltic dikelet which falls between tholeiitic and alkali fields (Fig. 5).

Four groups have been distinguished on the basis of the REE chondrite [Sun and Mc Donough, 1989] normalized patterns (Fig. 6). These four groups are also evident in the Primitive Mantle normalized patterns for moderately to highly incompatible elements (Spiderdiagrams of Fig. 6):

The group 1 exhibits flat REE patterns ( $[La/Yb]_N = 1.14$  to  $1.84$ ). this group is formed by the sill cores (Fig. 6A), the clinopyroxene (Fig. 6B), the doleritic pillow basalts (Fig. 6C) and the felsic rock (Fig. 6D) from the PSB pass and most of the sills cores from Visp (Va-5 and Va-11 in Fig. 6H). This REE pattern is typical of tholeiitic melts of Transitional-MORB (T-MORB) affinity [Sun and Mac Donough, 1989]. The clinopyroxene and their gabbroic host rock show similar REE patterns. This indicates that REE were not mobile during the metamorphism. On the spiderdiagram, the group 1 also displays a flat pattern (Fig. 6A, 6B, 6C, 6D and 6H). Nonetheless, pillow basalts (Fig. 6C) are Ta, Zr and Hf-enriched and most of the sill cores exhibit U-enrichment. Furthermore, the sill cores from the PSB pass show HFSE contents higher than those from Visp locality (Fig. 6A and 6H). Clinopyroxene is depleted in Th, U, Nb, Zr and Hf but the host rock is less depleted in Nb, Zr and Hf. In the Ti/Y versus Zr/Y diagram (Fig. 7), the sill cores fall near the Mantle Array, a result that confirms the MORB affinity of the group 1.

The group 2 is formed of two gabbroic sills from Visp with depleted LREE patterns ( $[La/Yb]_N = 0.67$  to  $0.82$ ). These two sills (Fig. 6H) are the less LFSE-enriched rocks and thus show N-MORB affinities [Sun and Mac Donough, 1989].

The doleritic sill margins (Fig. 6E) are more enriched in LREE ( $[La/Yb]_N = 4.8$  to  $16.2$ ). These REE patterns are similar to those of the black shales (Fig. 6F). The spiderdiagrams of the sill margin (Fig. 6E) are also similar to those of the black shales (Fig. 6F). In the Ti/Y versus Zr/Y diagram (Fig. 7), the sill margins and the black shales exhibit similar ratios to those of the post Archean schist [Brewer et al. 1992]. Moreover, the Sm/Nd ratios (0.18 to 0.25) of the sill margins are similar to those proposed by [Faure, 1986] for the black shales (Sm/Nd = 0.18) and pelites (Sm/Nd = 0.21). Thus, the chemical composition of sill margins could likely be related to assimilation of sediments during the sill intrusion into unconsolidated pelitic sediments.

The basaltic dikelet that intrudes the gneiss shows the highest LREE enrichment ( $[La/Yb]_N = 18$ ) (Fig. 6G) and the lowest Heavy Rare Earth Elements (HREE) abundances. Its spiderdiagram (Fig. 6G) is characterized by the lowest HFSE concentrations and by Th, U, Ta, Hf and Gd-enrichments. Th and U concentrate in the upper crust [Rollinson, 1993] and these high Th and U contents could be related to crustal contamination with the host rocks. However, the alteration of the sample (LOI > 10 wt %) could be responsible for a part of these element enrichments.

In summary, the tholeiitic rocks (whole rocks and clinopyroxene) of the Versoyen Complex show flat REE patterns and their incompatible trace element abundances fall between N-MORB and T-MORB. This intermediate range could be explained in two ways: variation of the mantle source or different ratios of partial melting.

The chilled margins of the sills are LREE enriched compared to their cores. This enrichment is related to contamination when hot mafic magmas intruded unconsolidated sediments rich in water. The geochemistry of the basaltic dikelet intruded in the gneiss remnant is contaminated by continental crust.

### **Nd and Sr isotopic compositions**

An age of 337 Ma has been taken to calculate the initial Sr and Nd ratios (Table 4) in agreement with the U/Pb age of Bussy et al. [2005] and Masson et al. [in press]. In the  $\epsilon_{Sr}$ - $\epsilon_{Nd}$  diagram (Fig 8), the

tholeiitic rocks (excluding the doleritic margins) show a wide range (+13.2 up to +74) of positive  $\epsilon_{\text{Sr}}(T=337 \text{ Ma})$  ratios. Acid leaching of the clinopyroxene did not change significantly its  $\epsilon_{\text{Sr}}$  ratio compared to that of the host rock. The shift of the  $\epsilon_{\text{Sr}}$  ratios towards high values reflects radiogenic Sr enrichments during the alteration and the metamorphism of the Versoyen Complex. Therefore, the  $\epsilon_{\text{Sr}}$  ratio cannot reflect the mantle source composition. Nonetheless, the very low values for the doleritic margins express the contamination by the black shales during the sill emplacement.

The  $\epsilon_{\text{Nd}}(T=337 \text{ Ma})$  ratios are more reliable because Nd-Sm are less mobile than Rb-Sr during alteration and metamorphism. These ratios provide significant information about the magma sources and the crustal contamination. The  $\epsilon_{\text{Nd}}$  ratios show a wide range of values from -9.9 to +9.

Most of the samples of the group 1 defined from the trace element study (sill cores, pillow basalts, felsic rock and gabbro) exhibit high  $\epsilon_{\text{Nd}}$  ratios which fall in the range of N-MORB.

The clinopyroxene and their gabbroic host rocks respectively exhibit  $\epsilon_{\text{Nd}}$  ratios of +8.6 and +7.4. This difference between the clinopyroxene and the host rocks cannot be related to alteration or metamorphic processes because both mineral and host rock show similar REE patterns. It rather suggests a contamination process that occurred after the crystallization of the clinopyroxene and during the late stage of the magmatic evolution. The contamination could be explained by an assimilation process of the wall of the sills during the cooling of the magma.

One sill core (Va-11) and two pillow basalts (92-24 and 92-42) show  $\epsilon_{\text{Nd}}$  ratios between +5 to +7. These values are lower than those of N-MORB but fall within the range of Oceanic Island Basalts (OIB) [De Paolo, 1989].

The sill margins show the lowest  $\epsilon_{\text{Nd}}$  ratios (-7.7 and -9.9) which correlate with the highest Th contents (13 and 18 ppm). This confirms that the sill margins assimilated sediments during their emplacement.

Finally, the basaltic dikelet displays an  $\epsilon_{\text{Nd}}$  ratios of + 1.2. Thus, this basalt likely derived from a mantle source which has suffered crustal contamination.

In the plot of  $\epsilon_{\text{Nd}}$  ratio versus Sm/Nd, the tholeiitic rocks fall between the N-MORB and OIB fields (Fig. 9). The sill core with the lowest  $\epsilon_{\text{Nd}}$  ratios (+5.6), shows a Sm/Nd ratio similar to OIB. Moreover, their high Zr/Ti and Zr/Y ratios (Fig. 7) approach those of OIB. The clinopyroxene and

the sill cores with  $\epsilon_{\text{Nd}}$  ratios of +9 have high Sm/Nd ratios and low Zr/Ti and Zr/Y ratios similar to those of N-MORB. This wide range of values for the tholeiitic rocks suggest a mixing of N-MORB and OIB sources. However, a contamination related to assimilation of sediments cannot be excluded.

## **DISCUSSION**

### **Nature of the mantle source of the Versoyen tholeiites**

Almost all the igneous rocks of the Versoyen Complex are N-MORB tholeiites. The trace element and Nd isotopic compositions of the Versoyen tholeiites suggest that these rocks were either generated by the mixing of two mantle sources (N-MORB and an OIB) or by the sediment assimilation during the sill emplacement.

The igneous rocks of the Versoyen Complex have been considered by numerous workers [Loubat, 1968; Schurch, 1987; Stampfli, 1993] as an ophiolitic suite because of the presence of serpentinized ultramafic associated with gabbros, dolerites and pillow basalts.

Nonetheless, in the PSB pass area, the tholeiitic rocks of the Versoyen Complex do not show the characteristics of ophiolitic suites generated by sea floor spreading along mid-oceanic ridge because: (i) The magmatism is reduced to mafic sills and pillow basalts rocks emplaced within crustal-derived sediments; (ii) Diabase dikes or layered gabbros are absent; (iii) Sediments are crustal-derived and differ significantly from the siliceous-rich and/or Fe- and Mn-rich pelagic sedimentary rocks deposited on ocean floor; (iv) The serpentinites do not show metamorphic textures developed under mantle conditions; (v) Locally basaltic dikelets are intruded in leucocratic gneisses (Fig. 3) and are affected by a crustal contamination. These five features suggest that the tholeiitic magma was emplaced in a basin in the vicinity of a continent. In the Visp locality, the basic complex presents more similarities with ophiolitic suites, because serpentinized peridotites show blastomylonitic textures and siliceous metasedimentary levels are present within the black shales. In this locality, the basic Complex could be generated by sea floor spreading. Thus, the oceanic basin appears to widen eastward and this basin does not seem to extend south-westward beyond the Tarentaise valley.

### **Age and origin of the Versoyen ocean**

The ages measured on Zircons of the Versoyen Complex appear very different from the late Mesozoic age usually admitted for the Versoyen Complex but are slightly dispersed. U-Pb data obtained on four felsic rocks [Schärer et al., 2000] show that zircons in this intrusion are composed of two components: (1) Archean, about 3.24 Ga old primary grains and (2) zircons that have re-crystallized at ~309 Ma, overgrowing old grains. Such a pattern substantiates that the dike magma was formed in Carboniferous times including melts derived from very old continental crust material.

The crystallisation ages obtained where the main gabbroic body intruded into the Versoyen series is 337 Ma [Bussy et al., 2005], but the outer rims of few zircons give ages down to about 300 Ma, that could be ascribe to a slight loss during metamorphism. Therefore, the difference in age between the two studies is not meaningful. Furthermore, the zircon bearing felsic rock shares with the Versoyen tholeiites similar trace element and Nd compositions, suggesting that this felsic rock is synchronical with the Versoyen tholeiites.

Therefore, a Visean age (~337 Ma) can probably be assigned to both the igneous components and intruded unconsolidated sediments of the Versoyen Complex and the Versoyen Complex is linked to the evolution of the Variscan domain.

From the Late Visean and up to the Early Permian, the Variscan belt is characterized by a Complex story involving both convergence [Franck and Oncken, 1990] and syn to post-thickening crustal extension [Ménard and Molnar, 1988]. This extension leads to crustal thinning and emplacement of within-plate calc-alkali and shoshonitic magmas [Ouazzani and Lapierre, 1986; Menot, 1987; Finger et al., 1990; Schaltegger, 1997]. The collapse of the orogen expended northward over time [Praeg, 2004]. Moreover, Stampfli [1996] show that Carboniferous basins may be related to major strike-slip ductile faults.

During the Visean, large volumes of shoshonitic diorites, monzonites, syenites and granites commonly associated with high -K mafic rocks, were formed within a zone extending parallel to the variscan orogen axis [Schaltegger, 1997]. The generation of the plutonic bodies was associated with N 30-40°striking, sinistral wrench-zones [Edel et al., 2007] and with an extensional event leading to continental basin opening [Bruguier et al., 1998]. A plate model for the Paleozoic [Stampfli and Borel,



2002] suggests that slab rollback of the northward subduction of PaleoTethys could produce a general collapse of the pre-existing Variscan cordillera and large-scale lateral displacement. Thus, the opening of the Versoyen oceanic basin does not seem to be linked to a major oceanic stage development. From the comparison of the PSB and Visp area, the oceanic domain appears to widen eastward and does not seem to extend south-westward beyond the Tarentaise Valley. Furthermore, the paleo-reconstruction of Pfiffner [1992] would suggest that the Versoyen domain extends toward the South West in the alpine "Zone Houillère".

Therefore we suggest an interpretation where the Versoyen tholeiites emplaced during the last stages of the crustal thinning context, or above an oceanic crust developed in a pull-apart basin located along a major Variscan wrench-fault zone. This interpretation looks like the Loubat and Delaloye [1984] or the Schmid et al. [1990] one, but involve quite different timing of the tectonics events.

The presence of Paleocene-Eocene radiolarians [Bousquet et al., 2002] close to mafic rocks derived from oceanic lithosphere [Durr et al., 1993] in lesser Pennine ophiolites suggests that the classically so-called Valaisan domain of the Alps is a mix, from East to West, of different domains with various Alpine and pre-Alpine evolutions. The present-day continuity at the scale of the Alps of the boundary between the Internal Alps and the External Alps (base of the lower Pennine in central Alps, and Western boundary of the Briançonnais domain in western Alps) would be basically inherited from the Variscan story but does not imply an Alpine evolution identical from North to South.

### **Geodynamic implications for the Alpine story**

Numerous works are still necessary to integrate the Carboniferous development of the Versoyen Complex in the tectonic models of the Alpine chain. We would like to emphasise at least the three following points:

*Structural reactivation at the boundary between Internal and External Alps* The boundary between Internal and External Alps is a major structure of the Alps and is characterised by a complex reactivation story: Variscan initiation of an oceanic domain, Mesozoic extension at the margin of the Neo-Tethys, initial alpine thrusting that lead to a burying at more than 60 km before 35Ma [Bousquet et al., 2002] and

probably before 45 Ma [Freeman et al., 1998; Fugenschuh and Schmid, 2003], ductile normal shearing at the foot-wall of the Briançonnais [Cannic et al., 1996; Bousquet et al., 2002] that lead to a rapid exhumation to a depth of  $\sim 40$  km before 27 Ma, and presumably between 31 and 27 Ma [Bousquet et al., 2002; Fugenschuh and Schmid, 2003], break-back-reactivation of the Basal Briançonnais thrust [Mugnier et al., 1993; Freeman et al., 1998] that possibly occurred around 12 Ma [Cannic et al., 1999] and less than 3 km normal fault displacement [Cannic et al., 1999] that is occurring after 5 Ma [Fugenschuh and Schmid, 2003]. Due to this complex story, we use the term "Pennine suture" [Mugnier and Marthelot, 1991] for the boundary between the Internal Alps and the external Alps.

*Can the Valaisan domain be a crustal-scale feature of the Western Alps?* The Valaisan oceanic domain is presently used to explain numerous intriguing data of the Alps: An entire Mesozoic ocean is considered as a key [Bousquet et al., 2002] to explain the westernmost eclogite facies of the Alps of the Valaisan domain. In the same way, a continuation of the domain located on the deep seismic Ecors profile between the two obvious reflection bands that cuts the upper crust is frequently inferred beneath the Grand-Paradiso at a depth of  $\sim 15$  km and is considered as the continuation of the units of a Valaisan ocean [Schmid and Kissling, 2000]. Though this geological interpretation of the deep seismic profile is fascinating, it seems to us an over-interpretation of geophysical data. We maintain the rational interpretation of this zone proposed by Cannic et al. [1999], and based on a coherency-weighted-migration procedure of the seismic sections [Mugnier and Marthelot, 1991]. The mean dip of the westernmost reflection band is smaller than the dip of the easternmost one, and the domain between the two reflection zone does not necessarily extend at depth along the flatter part of the suture. A detail interpretation of the reflections (Fig. 10) rather suggests that the BF is the most continuous structure is linked to the late extension along the BF and the BF cut through the PT. The boundary between the Valaisan flysh and the Mouthier unit is also cut through by the BF. Onlap-like reflection pattern occurs beneath the PT on to the top of the Mont-Blanc massif. This geometry does not preclude large (more than 60 km) alpine displacement along the Pennine suture, but precludes the extend of the "Valaisan domain" beneath the Internal domain.

*What is the Valaisan domain?* At the southern termination of the Valaisan domain, the Valaisan flysch, the Versoyen Complex and the Briançonnais domain of Vanoise have distinct pre-Mesozoic

substratums, respectively the sediments of "Permo- Houiller basin" in the Moutier unit [Antoine, 1971], an oceanic substratum and the lower "zone houillère" intruded by granite dated at 320 Ma [Freeman et al., 1998]. The three units (Flysh, Versoyen and lower "zone houillère") also show very distinct alpine metamorphic evolutions, with respectively greenschist peak, eclogitic peak [Cannic et al. 1996; Goffe and Bousquet, 1997] and blueschist or less peak [Freeman et al., 1998]. They are separated by tectonic contacts that are affected by a very complex Alpine story. Therefore, the substratum of the Valaisan flysch, the Versoyen Complex and the Briançonnais domains have been deposited in different paleogeographic settings and the restoration of their respective position remains highly conjunctural. It appears that the Valaisan domain, formed of the Versoyen Complex and Valaisan flysch, has no clear geological signification. And its definition at the scale of the Alps is a misleading concept.

In conclusion, our paper suggests that Variscan oceanic remnants are stretched along the Pennine suture. Therefore the Pennine suture is inherited from the pre-alpine story but the Briançonnais domain is a part of European plate. The structural Variscan heritage controls at lithospheric-scale the structural inversion of the European margin of the Tethys and the position of the greatest megathrust of the Alps at the boundary between internal and external Alps.

### **Remerciements:**

Les données géochimiques ont été acquises lors de la thèse de S. Cannic [1996] dirigée par H. Lapierre et J.L. Mugnier; leur remise en perspective par rapports aux nouveaux résultats acquis sur les Alpes a été effectué par J.L. Mugnier, à la mémoire de la regrettée H. Lapierre. Nous remercions Georges Mascle, Jean-Luc Epard et un relecteur anonyme pour leurs remarques extrêmement utiles.

## References

ANTOINE P. (1971).- La zone des brèches de Tarentaise entre Bourg-Saint-Maurice (vallée de l'Isère) et la frontière italo-suisse.- *PhD Grenoble*, 367 p.

ANTOINE P., LOUBAT H. & VATIN-PERIGNON N. (1973).- Hypothèses nouvelles sur la signification des "ophiolites" du domaine pennique externe (Savoie-Valais).- *Géol. Alpine*, **49**, 21-39.

BARBIER R. (1951).- La prolongation de la zone sub-Briançonnaise de France en Italie et en Suisse. Les conséquences pour une corrélation d'ensemble des zones penniques de ces trois pays.- *Trav. Lab. géol. Grenoble*, **29**, 3-46.

BERTRAND J., COURTIN B. & VUAGNAT M. (1982).- Elaboration d'un secteur de lithosphère océanique liguro-piemontais d'après les données de l'ophiolite de Montgenèvre (Hautes-Alpes, France et Province de Turin, Italie).- *Ophioliti*, **2/3**, 155-196.

BOCQUET J. (1974).- Etudes minéralogiques et pétrographiques sur les métasédiments d'âge alpin dans les Alpes françaises.- *PhD Grenoble*, 490 p.

BREWER T. S., HERG J. M., HAWKESWORTH C. J., REX D. & STOREY B. C. (1992).- Coast Land dolerites and the generation of Antarctic continental flood basalts. In: B. C. STOREY ALABASTER, T. & R. J. PANKHURST, Eds.- *Geol. Soc. Spec. Pub.*, London, 185-208.

BRUGUIER O., BECQ-GIRAUDON J.F., BOSCH, D. & LANCELOT J.R. (1998).- late Viséan hidden basins in the internal zones of the Variscan belt; U-pb zircon evidence from the French Massif Central.- *Geology*, **26**, 627-630.

BOUSQUET R., GOFFÉ B., VIDAL O., PATRIAT M., & OBERHÄNSLI R. (2002).- The tectono-metamorphic history of the Valaisan domain from the Western to the Central Alps: New constraints for the evolution of the Alps.- *GSA Bulletin*, **114**, 207-225.

BUSSY F., EICHENBERGER M., GIROUD M., MASSON H. , MEILHAC C. & PRESNIAKOV S. (2005)- Early Carboniferous age of the Versoyen magmatism and consequences: non-existence of a "Valais ocean".- in: *the Western Alps, 3th Swiss geoscience meeting, Zürich*, p. 58.

BUTLER R. (1984).- Balanced cross-section and their implications for the deep structure of the northwest Alps: discussion.- *J. Struct. Geol.*, **6**, 603-606.

CANNIC S. (1996).- L'évolution magmatique et tectono-métamorphique du substratum du domaine Valaisan (Complexe du Versoyen, Alpes occidentales): implications dans l'histoire alpine.- *PhD, Grenoble*, 215 p.

CANNIC S., LARDEAUX J.-M., MUGNIER J.-L. & HERNANDEZ J. (1996).- Tectono-metamorphic evolution of the Roignais-Versoyen Unit (Valaisan domain, France).- *Eclogae geol. Helv.*, **89**, 321-343.

CANNIC S., MUGNIER J.-L. & LARDEAUX J.-M. (1999).- Neogene extension in the Western Alps.- *Mémoire Science geol.*, **51**, 33-45.

CARRUPT E. (2003).- New stratigraphic, structural and geochemical data from the Val Formazza-Binntal area (Central Alps).- *Mémoire Géol. (Lausanne)*, **41**, 118 p.

COLOMBI A. & PFEIFER H. R. (1986).- Ferrogabroic and basaltic meta-eclogites from the Antrona mafic-ultramafic complex and the Centovalli-Locarno region (Italy and Southern Switzerland)- first results.- *Schweiz. mineral. petrogr. Mitt.*, **66**, 99-110.

COLOMBI A. (1989).- Métamorphisme et géochimie des roches mafiques des Alpes ouest-centrale (geoprofil Viege-Domodossola-Locarno).- *Mem. Soc. geol. Lausanne*, **4**, 156 p.

De Paolo D. J. [1988].- Neodymium Isotope Geochemistry.- *Minerals and Rocks, Berlin, Heidelberg, New-York, Eds*, 187 p.

DIETRICH V. & OBERHANSLI R (1975).- Die pillow-laven des Vispertales.- *Schweiz. Mineral. Petrogr. Mitt.*, **55**, 79-87.

DURR S., RING. U. & FRISCH W. (1993).- geochemistry and geodynamic significance of north Penninic ophiolites from the Central Alps.- *Schweizerisches mineralogische and Petrographische Mitteilungen*, **73**, 407-419.

EDEL J.-B., SCHULMANN K., ROTSTEIN Y. (2007).- The Variscan tectonic inheritance of the upper Rhine Graben: evidence of reactivations in the Lias, late Eocene-Oligocene up to the recent.- *International Journal of Earth Sciences*, **96**, 305-325.

FAURE G. (1986).- The Sm-Nd method of dating. *In: Principles of Isotope Geology-. Second edition, John Wiley and Sons, New York, 239-248.*

FINGER F. & STEYRER H. P. (1990).- I-type granitoids as indicators of Late Paleozoic convergent ocean-continent margin along the southern flank of the central European Variscan orogen.- *Geology*, **18**, 1207-1210.

Franck W. and Oncken, O. 1990 Geodynamic evolution of the North-Central Variscides- a Comic Strip. *In: R. Frieman, P. Giese, and St Muleler, (eds) The European Geotraverse: Integrative studies, 187-194, European Science foundation, Strasbourg, France.*

FREEMAN S., BUTLER R., CLIFF, A., INGER S. & BARNICOAT A. (1998).- deformation migration in an orogen-scale shear zone array: an example from the Basal Briançonnais thrust, internal franco-Italian Alps.- *Geol. Mag.*, **135**, 349-367.

FRISCH, W. (1979).- Tectonic propagation and plate tectonic evolution of the Alps.- *Tectonophysics*, **60**, 121-139.

FUDRAL S. (1973).- Contribution à l'étude de le l'unité de Moutiers entre le torrent du Cornet d'Arèches et le hameau des Chapieux.- *PhD Grenoble*, 129 p.

FUGENSCHUH, B., LOPRIENO, A., CERIANI, S. & SCHMID, S. (1999).- Structural analysis of the Subbriançonnais and Valais units in the area of Moutiers (Savoy, Western Alps): Paleogeographic and tectonic consequences.- *International Journal of Earth Sciences*, **88**, 201-218.

FUGENSCHUCH B. & SCHMID S. (2003).- late stage of deformation and exhumation of an orogen constrained by fission-track data: a case study in the Western Alps.- *GSA bulletin*, **115**, 1425-1440.

GELY J. P. (1989).- Stratigraphie, tectonique et métamorphisme comparés de part et d'autre du Front pennique en Tarentaise (Alpes de Savoie, France).- *PhD Chambery*, 343 p.

GOFFÉ B. & BOUSQUET R. (1997).- Ferrocapholite, chloritoid and lawsonite in metapelite of the Versoyen and Petit-SaintBernard units (Valaisan zone, Western Alps).- *Schweiz. Mineral. Petrogr. Mitt.*, **77**, 137-148.

JEANBOURQUIN P. & BURRI M. (1991).- Les métasediments du Pennique inférieur dans la région de Brigue-Simplon. Lithostratigraphie, structure et contexte géodynamique dans le bassin Valaisan.- *Eclogae geol. Helv.*, **84**, 463-481.

JEANBOURQUIN P. (1994).- The lower Penninic nappes in the Western Alps: The link between Helvetic and Penninic.- *J. Struct. Geol.*, **16**, 895-898.

LAGABRIELLE Y. (1987).- Les ophiolites : marqueurs de l'histoire tectonique des domaines océaniques.- *PhD. Thesis Brest*, 350 p.

LASSERRE J. L. & LAVERNE C. (1976).- Le volcanisme tholéiitique de la zone du Versoyen (Alpes franco-italiennes): minéralogie, pétrographie et géochimie.- *PhD Grenoble*, 252 p.

LEMOINE M. (1980).- Serpentinites, gabbros and ophicalcites in the Western Alps: possible indicators of oceanic fracture zones and associated protusions in the Jurassic-Cretaceous Thetys.- *Archives des Sciences de Genève*, **33**, 103-115.

LETERRIER, J., MAURY R. C., THONON P., GIRARD D. & MARHAL M. (1982) .- Clinopyroxene composition as a method of identification of the magmatic affinities of paleo-volcanic series.- *Earth Planet. Sci. Lett.*, **59**, 139-154.

LOUBAT H. (1968).- Etude pétrographique des ophiolites de la "zone du Versoyen" Savoie (France). Province d'Aoste (Italie).- *PhD, Archives des Sciences de Genève*, **28**, 247-265,.

LOUBAT H. & DELALOYE M. (1984).- La zone du Versoyen (Alpes franco-italiennes): le témoin d'une océanisation mésozoïque circonscrite constituant un milieu hybride, subvolcano-sédimentaire avec mobilisats et adinoles.- *Geol. Alpine*, **60**, 45-76.

MASSON H. (2002).- Ophiolites and other (ultra)basic rocks from the West-Central Alps: new data for a puzzle.- *Bull. Géol. Lausanne*, **356**, et *Bull. Soc. Vaudoise Sci. Nat.*, **88/2**, 263-276.

MASSON H., BUSSY F., EICHENBERGER M., GIROUD N., MEILHAC C & PRESNIAKOV S. (in press).- Age carbonifère des ophiolites du Versoyen et conséquences pour la géodynamique des Alpes occidentales.- *Bulletin de la Société Géologique de France*, **this volume**.

MENARD G. & MOLNAR P. (1988).- Collapse of a Hercynian Tibetan Plateau into a late Pleozoic European Basin and Range province.- *Nature*, **334**, 235-237.

MENOT R. P. (1987).- Magmatisme paléozoïque et structuration carbonifère du massif de Belledonne (Alpes françaises). Contraintes nouvelles pour les schémas d'évolution de la chaîne varisque Ouest-Européenne.- *Ph. D. Thesis, Lyon, Rennes*, 465 p.

MUGNIER J.L. & MARTHELOT J.M. (1991).- Crustal reflections beneath the Alps and the Alpine foreland: Geodynamic implications. *in: continental lithosphere : deep seismic reflections.- A. G. U. Geodynamic Series*, **22**, p. 177-183

MUGNIER J.L., LOUBAT H. & CANNIC S. (1993).- Correlation of seismic image and geology at the boundary between internal and external domains of the western Alps.- *Bull. Soc. Géol. France*, **164**, 697-708.

NISBET E. G. & PEARCE J. A. (1977).- Clinopyroxene composition in mafic lavas from different tectonic settings.- *Contrib. Miner. Petrol.*, **63**, 149-160.

OUAZZANI H. & LAPIERRE H. (1986).- Le magmatisme carbonifère de la zone Briançonnaise (Alpes internes). Essai sur la lecture des magmatismes calco-alcalins tardifs dans les chaînes de collision continentale.- *C.R. Acad. Sci. Paris*, **302**, 1171-1176.

PAVONI N. (1961).- Faltung durch horizontal verschiebung.- *Eclogae Geol. Helv.*, **54**, 515-534.

PEARCE J. A. (1982).- Trace element characteristics of lavas from destructive plate boundaries. *In: R. S. Thorpe, Eds.- Wiley and sons, Chichester*, 525-547.

PFIFFNER A. (1992).- Alpine Orogeny.- *in: a continent revealed-the European Geotraverse*, BLUNDELL D., FREEMAN R. & MUELLER S. Eds.- *University Press, Cambridge*, 180-190.

PRAEG D. (2004).- Diachroneous Variscan late-orogenic collapse as a response to multiple detachments: a view from the internides in France to the foreland in the Irish sea.- *Geological Society Special Publications, London*, **223**, 89-138.



ROSENBAUM G. & LISTER G. (2005).- The Western Alps from the Jurassic to Oligocene: spatio-temporal constraints and evolutionary reconstructions.- *Earth-Science Reviews*, **69**, 281-306.

ROLLINSON H. (1993).- Using Geochemical Data: Evaluation, Presentation, Interpretation- *Longman Scientific and Technical, Essex*, 352 p.

SCHALTEGGER U. (1997).- magma pulses in the central Variscan belt: episodic melt generation and emplacement during lithospheric thinning.- *Terra Nova*, **9**, 242-245.

SCHARER U., CANNIC S.& LAPIERRE H. (2000).- Preliminary evidence for a Hercynian age of the Versoyen complex, western Alps.- *C.R. Acad. Sci. Paris*, **330**, 325-332.

SCHMID S., RUCK P. & SCHREURS G. (1990).- The significance of the Schams nappes for the reconstruction of the paleotectonic and orogenic evolution of the Penninic zone along the NFP-20 east traverse (Grisons, eastern Switzerland).- *Mémoire de la Société Géologique de France*, **156**, 263-287.

SCHMID S. & KISSLING E. (2000).- The arc of the Western Alps in the light of geophysical data on deep crustal structure.- *Tectonics*, **19**, 62-85.

SCHOELER H. (1929).- La nappe de l'Embrunais au nord de l'Isère.- *Bull. Carte geol. France* **175**, 422 p.

SCHURCH M. F. (1987).- Les ophiolites de la zone du Versoyen: témoin d'un bassin à évolution métamorphique complexe.- *PhD, Genève*, 153 p.

STAMPFLI G. M. (1993).- Le Briançonnais, terrain exotique dans les Alpes ?.- *Eclogae geol. Helv.*, **86**, 1-45.

STAMPFLI, G. (1996).- The Intra-Alpine terrain: A Paleotethyan remnant in the Alpine Variscides.- *Eclogae geol. Helv.*, **89**, 13-42.

STAMPFLI G. & BOREL G. (2002).- a plate tectonic model for the Paleozoic and Mesozoic constrained by dynamic plate boundaries and restored synthetic oceanic isochrones.- *Earth and Planetary Science Letters*, **196**, 17-33.

STECK A. (1990).- Une carte des zones de cisaillement ductile dans les Alpes Centrales.- *Eclogae geol. Helv.*, **83**, 603-627.

SUN S. S. & MAC DONOUGH W. F. (1989).- Chemical and isotopic systematics of oceanic basalts: Implication for mantle composition and processes. *In: Magmatism in the ocean basin - Geol. Soc. Spec. Pub.*, **42**, 313-345.

TRUMPY R. (1955).- Remarques sur la corrélation des unités penniques externes entre la Savoie et le Valais et sur l'origine des nappes prealpines.- *Bull. Soc. Geol. France*, **6**, 217-231.

WASSERBURG G. J., JACOBSEN S. B., DE PAOLO D. J., MC CULLOCH M. T. & WEN T. (1981).- Precise determination of Sm/Nd ratios, Sm and Nd isotopic abundance in standard solutions.- *Geoch. Cosmoch. Acta*, **45**, 2311-2323.

Sample	93-16						92-18			95-23		93-43
<b>SiO<sub>2</sub></b>	51.11	50.54	50.28	48.85	49.72	52.79	51.85	51.76	52.07	50.24	51.01	50.87
<b>Al<sub>2</sub>O<sub>3</sub></b>	2.83	3.12	3.19	3.41	3.23	1.94	2.06	2.00	2.23	3.02	2.83	2.49
<b>TiO<sub>2</sub></b>	1.04	1.31	1.38	2.12	1.98	0.58	0.64	0.62	0.69	0.98	0.88	0.93
<b>FeO</b>	5.84	5.91	6.24	6.51	6.22	5.22	5.81	5.87	5.65	6.49	6.24	6.7
<b>MgO</b>	14.88	15.82	15.93	15.78	15.82	16.4	16.95	16.87	16.13	16.08	15.95	15.53
<b>CaO</b>	21.12	20.9	20.65	20.82	20.74	21.42	20.3	20.68	21.44	21.02	20.76	20.96
<b>MnO</b>	0.16	0.16	0.19	0.22	0.16	0.2	0.17	0.26	0.19	0.22	0.09	0.22
<b>Cr<sub>2</sub>O<sub>3</sub></b>	0.43	0.68	0.76	0.32	0.33	0.52	0.64	0.71	0.63	0.6	0.66	0.24
<b>NiO</b>	0.01		0	0	0	0.09	0.05	0.12	0.01	0.08	0.00	0.03
<b>Na<sub>2</sub>O</b>	0.64	0.39	0.46	0.43	0.41	0.47	0.36	0.32	0.36	0.44	0.31	0.37
<b>Σ</b>	98.06	98.83	99.08	98.46	98.61	99.63	98.83	99.21	99.4	99.17	98.73	98.34
<b>S i</b>	1.91	1.88	1.86	1.82	1.85	1.94	1.92	1.91	1.92	1.86	1.90	1.90
<b>ALIV</b>	0.08	0.12	0.13	0.17	0.14	0.06	0.08	0.09	0.07	0.14	0.10	0.09
<b>AlVI</b>	0.04	0.01	0.00	0.00	0.00	0.02	0.01	0.00	0.02	0.00	0.02	0.01
<b>Ti</b>	0.03	0.04	0.04	0.06	0.05	0.02	0.02	0.02	0.02	0.03	0.03	0.03
<b>Mg</b>	0.83	0.88	0.88	0.88	0.88	0.90	0.94	0.93	0.89	0.89	0.89	0.87
<b>Fe 3+</b>	0.02	0.04	0.06	0.1	0.06	0.02	0.04	0.06	0.03	0.11	0.03	0.05
<b>Fe 2+</b>	0.17	0.14	0.13	0.10	0.14	0.14	0.14	0.12	0.15	0.09	0.16	0.16
<b>Ca</b>	0.85	0.83	0.82	0.83	0.83	0.84	0.81	0.82	0.85	0.83	0.83	0.84
<b>Mn</b>	0.01	0.01	0.01	0.01	0.01	0.01	0.01	0.01	0.01	0.01	0.00	0.01
<b>Cr</b>	0.01	0.01	0.02	0.01	0.01	0.02	0.02	0.02	0.02	0.02	0.02	0.01
<b>Na</b>	0.05	0.03	0.03	0.03	0.03	0.30	0.03	0.02	0.03	0.03	0.02	0.03
<b>En</b>	45	46	46	46	46	47	49	48	46	46	46	45
<b>Fs</b>	10	10	10	11	10	8	9	9	9	10	10	11
<b>Wo</b>	45	44	44	43	44	45	42	43	45	44	44	44

Table 1: Representative clinopyroxene compositions of the Versoyen complex igneous rocks.

Formula based on 6 oxygens. Microprobe analyses were carried out at the Laboratoire de Micro Analyse Electronique, Université de Lausanne (Switzerland), on a CAMEBAX microprobe operating at 15 KV, 15 nA and using natural minerals as standards. The integration time was 20 s.

Tableau 1: Composition des clinopyroxènes du complexe du Versoyen. (Formule basée sur 6 oxygènes). Les analyses ont été réalisées au Laboratoire de Micro Analyse Electronique, Université de Lausanne (Suisse) sur la microsonde CAMEBAX opérant à 15 KV, 15 nA et utilisant des minéraux naturels comme standards. Les données sont moyennées sur 20 s.

Location	Core of sills						Pillow-basalts				Felsic rock	Dikelets	
Sample	92-18	92-19	92-35	93-16	95-23	95-23	92-10	92-22	92-24	92-42	94-104	93-02	94-62
Facies	MG2	MG2	MG2	MD2	MG3	Cpx3	MD1	MD1	MD1	MD2	FR	MB2	MB
SiO <sub>2</sub>	47.84	49.81	49.46	44.56	-	-	51.06	50.95	52.2	40.32	48.65	30.52	30.66
TiO <sub>2</sub>	2.08	2.75	2.04	1.87	-	-	1.95	2.02	2.04	2.12	2.15	0.09	0.1
Al <sub>2</sub> O <sub>3</sub>	14.5	13.51	15.21	14.88	-	-	14.86	16.51	15.73	14.73	16.66	17.36	17.2
Fe <sub>2</sub> O <sub>3</sub>	12.21	13.28	10.58	9.32	-	-	10.5	8.71	8.24	8.6	10.53	19.38	17.35
MnO	0.2	0.2	0.32	0.4	-	-	0.28	0.14	0.13	0.71	0.19	0.23	0.27
MgO	8.53	4.97	6.94	6.84	-	-	7.59	5.25	4.08	4.41	7.04	20.3	23.2
CaO	7.03	8.53	4.91	8.03	-	-	4.49	8.5	10.16	12.13	7.9	1.15	0.57
Na <sub>2</sub> O	3.75	4.44	3.54	4.51	-	-	5.44	4.8	5	5.33	3.82	Traces	Traces
K <sub>2</sub> O	Traces	Traces	Traces	Traces	-	-	Traces	0.35	0.03	Traces	0.03	Traces	0.02
P <sub>2</sub> O <sub>5</sub>	0.3	0.34	0.26	0.25	-	-	0.26	0.34	0.34	0.38	0.25	0.1	0.08
LOI	3.38	1.99	6.59	9.14	-	-	3.37	2.17	1.84	11.05	2.8	10.76	10.45
Σ	99.82	99.82	99.78	99.8	-	-	99.8	99.74	99.79	99.78	100.02	99.89	99.9
Ni ppm	166	37	77	56	162	139	74	82	66	45	123	566	439
Cr	206	157	212	217	1958	1570	199	189	145	173	147	3.78	3.01
V	285	315	269	300	822	652	270	273	294	240	249	60	83.2
Y	39	55	37	42	74	67	34	37	37	43	37	6.1	-
Zr	158	250	158	133	92	50	162	188	178	206	191	97	151
Nb	4.53	7.60	5.91	3.5	11.4	1.58	<5	<5	13	6.8	6.09	9.8	9.24
Ba	4.43	6.2	16	29	23.2	8.38	<5	70	<5	4.71	23	11	1.3
Sr	170	125	127	290	214	207	197	329	453	312	310	9.93	0.85
Rb	0.47	1.41	0.77	0.97	0.96	0.29	5	14	5	0.51	0.56	4.91	4.67
Co	35	22	28	28	34	38	33	26	26	30	26	19	27
Zn	85	103	79	79	72	72	81	70	55	65	82	364	321
Cu	55	52	58	58	56	10.3	63	41	51	79	36	2.93	2.42
Zr/Ti	0.0125	0.0204	0.0096	0.0109	-	-	0.0138	0.0155	0.0145	0.0162	0.0148	0.1796	0.2517
Ti/Y	320	300	331	267	-	-	344	328	331	296	349	89	-
Zr/y	4.05	4.55	4.27	3.17	1.24	0.75	4.76	5.08	4.81	4.79	5.16	15.9	-
Nb/Y	0.12	0.14	0.15	0.08	0.15	0.024	<0.15	<0.13	0.35	0.16	0.16	1.61	-
La	7.1	10.00	6.40	7.5	8.48	7.92	7.51	9.8	9.28	7.3	8.87	17.1	-
Ce	21	29	19.40	22	26.2	24.5	22	27	22	19	25	35	-
Pr	3.43	4.85	3.14	3.56	4.46	4.13	-	-	-	3.1	3.64	4.15	-
Nd	17.7	25.00	16.6	18.6	24.64	22	17.25	19.11	16.03	16.1	17.71	14.9	-
Sm	5.4	7.60	4.96	5.46	8.4	7.32	5.57	5.99	5.64	5.3	5.03	3.02	-
Eu	2.04	2.72	1.59	1.98	3.26	2.82	1.72	1.87	1.68	1.77	1.73	0.4	-
Gd	7.2	9.44	6.39	7.03	10.98	10.1	5.68	5.79	5.87	7.5	6.45	2.54	-
Dy	7.9	10.57	6.95	7.74	13.98	11.24	6.87	7.08	6.84	8.9	6.9	1.33	-
Ho	1.68	2.18	1.43	1.62	2.82	2.43	-	-	-	1.88	1.39	0.16	-
Er	4.8	5.60	3.68	4.15	8.04	6.88	4.16	3.98	3.68	5.3	4.23	0.45	-
Yb	4.48	5.69	3.44	3.92	7.14	6.13	4.21	4.07	3.62	4.88	3.74	0.68	-
Lu	0.67	0.83	0.51	0.6	0.96	0.92	0.65	0.65	0.63	0.71	0.57	0.11	-
Hf	4.39	6.16	3.86	3.24	3.26	1.84	-	-	-	5.77	4.52	3.98	-
Ta	0.29	0.38	0.23	0.27	1.3	0.03	-	-	-	0.47	0.55	1.17	-
W	0.15	1.42	0.75	1.58	-	-	-	-	-	<0.10	-	1.43	-
Pb	3.97	6.70	4.90	6.5	3.8	2.27	-	-	-	4.94	4.01	9.4	-
Th	0.36	0.66	0.40	0.51	0.26	0.27	<5	<5	<5	0.41	1.14	17.58	-
U	0.1	0.37	0.1	0.16	0.6	0.06	-	-	-	0.1	0.3	2.94	-
Sm/Nd	0.31	0.32	0.30	0.29	0.34	0.33	0.32	0.31	0.35	0.33	0.28	0.2	-
(La/Yb) <sub>N</sub>	1.14	1.26	1.33	1.37	0.85	0.93	1.28	1.73	1.84	1.07	1.70	18.04	-
Eu/Eu*	1.01	0.94	0.94	0.99	1.05	1.01	0.94	0.98	0.9	0.87	0.94	0.45	-

Table 2: Major and trace elements of igneous and sedimentary rocks of the Versoyen complex near the Petit Saint Bernard pass (PSB). MG: Metagabbros, FG: Flasergabbros, MD: Metadolerites, MB: Metabasalts, FR: Felsic rock.

Tableau 2: Éléments majeurs et traces des échantillons (sédiments et roches ignées) du Complexe du Versoyen à proximité du col du petit saint Bernard. MG: Métagabbros, FG: "Flasergabbros", MD: Métadolerites, MB: Métabasalts, FR: roches riches en feldspaths.

Location	Margin sills				Black shales			Core of sills			
Sample	92-06	92-12	92-16	92-21	94-96	94-93	95-26	VA5	VA 11	VA 12	VA 16
Facies	MD1	MD2	MD1	MD2	MS3	MS3	MS3	MG3	MD3	MG3	FG3
SiO <sub>2</sub>	53.24	48.81	48.78	58.75	52.56	54.12	57.52	47.23	49.38	49.82	50.26
TiO <sub>2</sub>	1.08	0.44	1.38	0.68	0.72	0.89	0.9	1.44	1.42	1.57	1.7
Al <sub>2</sub> O <sub>3</sub>	21.26	10.5	15.66	17.76	17	20.1	20.93	14.96	16.29	14.93	14.98
Fe <sub>2</sub> O <sub>3</sub>	7.19	5.84	8.14	7.69	5.3	6.76	7.82	9.66	10.2	9.52	8.89
MnO	0.14	1.12	0.39	0.22	0.39	0.24	0.26	0.13	0.15	0.15	0.13
MgO	3.75	2.41	3.97	3.2	2.94	3.82	2.78	6.36	6.76	5.61	5.77
CaO	1.51	13.57	7.83	1.31	8.17	3.2	0.11	12.59	9.1	9.17	9.84
Na <sub>2</sub> O	6.75	3.32	3.47	5.8	1.16	0.86	0.77	3.08	2.75	4.92	4.64
IC <sub>2</sub> O	1.47	0.4	1.33	1.27	2.06	3.19	3.59	0.15	0.71	0.52	0.19
P <sub>2</sub> O <sub>5</sub>	0.08	0.39	0.2	0.19	0.25	0.24	0.16	0.24	0.21	0.24	0.22
LOI	3.3	12.78	8.6	2.93	9.28	6.36	4.99	3.98	2.86	3.4	3.23
Σ	99.77	99.58	99.75	99.8	99.83	99.78	99.82	99.82	99.83	99.85	99.85
Ni ppm	56	45	84	72	76	91.6	93.4	111	48.8	86.1	33.6
Cr	172	65	159	126	124	134	132	324	287	235	314
V	216	69	200	144	139	170	166	316	246	269	305
Y	28	33	32	26	31	25	18.49	35.1	32.4	35.1	34.7
Zr	174	77	142	123	132	165	573	115	133	120	136
Nb	15	15.4	18	17.6	18	21.9	21.5	4.3	4.1	4.4	5.2
Ba	215	69	16	286	190	352	382	14	92.5	33.8	13.7
Sr	137	329	162	77	131	94	68.9	235	178	167	135
Rb	61	24	63	68	102	160	188	3.3	23.9	12.6	4.7
Co	9.00	13	26	26	20	26.3	18.6	41.9	37	30.5	33.6
Zn	83	100	49	37	62	57.6	135	78.2	95.3	72.5	65.8
Cu	10	33	19	11	-3.2	7.8	48.2	58	18.8	65.6	41.8
Zr/Ti	0.0268	0.0292	0.0171	0.0301	0.0305	0.0308	0.1062	0.0133	0.0156	0.0127	0.0133
Ti/Y	231	80	259	157	140	214	292	246	263	268	294
Zr/Y	6.21	2.33	4.4	4.73	4.26	6.6	30.99	3.28	4.1	3.42	3.92
Nb/Y	0.54	0.47	0.56	0.68	0.59	0.87	1.16	0.12	0.13	0.13	0.15
La	59.31	38	23.77	38	39.88	35.07	37.5	5.87	7.87	3.06	3.6
Ce	129	92	46	83	86	78	83	16	20	10	12.3
Pr	-	10.4	-	8.6	8.56	7.85	8.12	2.51	2.91	1.85	2.23
Nd	49.24	44	24.54	33	31.91	28.72	29.71	13.37	14.51	10.51	11.85
Sm	9.62	8.8	6.19	6.05	5.67	5.12	5.04	4.11	4.06	3.58	3.98
Eu	2.54	1.97	1.63	1.46	1.72	1.03	1.08	1.54	1.39	1.21	1.38
Gd	7.9	8.4	6.85	5.5	5.54	4.69	4.05	5.24	4.91	4.82	5.23
Dy	6.25	6.8	6.11	4.98	5.11	4.53	3.5	6.54	5.98	6.41	6.68
Ho	-	1.27	-	1.01	1.04	0.89	0.7	1.31	1.21	1.32	1.38
Er	2.87	3.22	3.35	2.87	3.03	2.81	2.09	3.78	3.52	3.8	3.73
Yb	2.63	2.79	3.55	2.8	2.78	2.64	2.28	3.44	3.31	3.3	3.15
Lu	0.39	0.4	0.63	0.42	0.38	0.4	0.36	0.46	0.46	0.43	0.43
Hf	-	2.52	-	4.11	3.8	4.71	14.48	1.02	0.36	0.65	0.41
Ta	-	1.12	-	1.29	1.18	1.4	1.42	0.26	0.31	0.31	0.42
W	-	<0.1	-	1.12							
Ph	-	23	-	3.07	11.04	10.77	6.69	1.52	6.9	1.86	0.78
Th	18	8.5	<5	13.3	11.01	13.39	12.86	0.61	0.96	0.39	0.26
U	-	1.98	-	2.79	2.15	2.7	1.94	0.22	0.41	0.12	0.15
Sm/Nd	0.19	0.20	0.25	0.18	0.18	0.18	0.17	0.31	0.28	0.34	0.34
(La/Yb) <sub>N</sub>	16.18	9.77	4.8	9.73	10.29	3.53	11.80	1.22	1.70	0.67	0.82
Eu/Eu*	0.9	0.71	0.77	0.78	0.95	0.65	0.74	1.02	0.96	0.90	0.93

Table 3: Major and trace elements of igneous and sedimentary rocks of the Visp complex. MG- Metagabbros, FG- Flaser gabbros, MD- Metadolerites, MB- Metabasalts, MS- Metasediments.

Tableau 3: Eléments majeurs et traces des échantillons (sédiments et roches ignées) du Complexe basique à proximité de Visp. MG- Métagabbros, FG- "Flaser gabbros", MD- Métadolerites, MB- Métabasalts, MS- Métasédiments.

N°	Location	Sample	Sr	Rb	87Rb/86Sr	87Sr/86Sr norm	87Sr/86Sr (337Ma)	$\epsilon_{Sr}$ (337Ma)	Nd	Sm	147Sm/144Nd	143Nd/144Nd norm	143Nd/144Nd (337Ma)	$\epsilon_{Nd}$ (337Ma)
92-18	PSB	Gabbroic core	170	0.47	0.01	0.708000±26	0.70796	54.8	17.7	5.40	0.184	0.513038 ±4	0.51263	8.3
92-19	PSB	Gabbroic core	125	1.41	0.12	0.706632±10	0.70648	33.7	25	7.60	0.196	0.513026 ±7	0.51262	8.1
93-16	PSB	Doleritic core	290	0.97	0.02	0.706666±11	0.70661	35.7	18.6	5.46	0.177	0.513050 ±6	0.51266	8.9
95-23	PSB	Gabbroic core	214	0.96	0.01	0.706701±17	0.70664	36.0	24.6	8.4	0.198	0.513036 ±8	0.51258	7.3
95-23	PSB	Clinopyroxene	207	0.29	<0.01	0.706475±20	0.70646	33.4	22	7.32	0.152	0.513087 ±9	0.51264	8.6
92-10	PSB	Doleritic pillow	197	5	0.07	0.708616±13	0.70826	59.1	17.2	5.57	0.195	0.513049 ±5	0.51262	8.0
92-22	PSB	Doleritic pillow	329	14	0.12	0.707025±9	0.70643	33.1	19.1	5.99	0.189	0.513016 ±6	0.51260	7.7
92-24	PSB	Doleritic pillow	453	5	0.03	0.707136±12	0.70698	40.9	16	5.64	0.213	0.513027 ±5	0.51256	6.9
92-42	PSB	Doleritic pillow	312	0.51	<0.01	0.709355±4	0.70933	74.3	16.1	5.30	0.199	0.512982 ±6	0.51254	6.6
93-02	PSB	Basaltic dykelet	33	4.91	0.43	0.711378±24	0.70931	74.0	14.9	3.02	0.123	0.512557 ±7	0.51229	1.6
94-104	PSB	Felsic rock	310	0.56	0.01	0.707992±15	0.70797	54.9	17.7	5.03	0.172	0.513190 ±10	0.51281	11.8
92-06	PSB	Doleritic margin	137	61	1.29	0.710591±37	0.70441	4.4	49	9.62	0.118	0.512123 ±8	0.51186	-6.7
92-21	PSB	Doleritic margin	77	68	1.73	0.712085±14	0.69982	-60.8	24.1	6.30	0.158	0.512054 ±10	0.51171	-9.7
94-93	PSB	Black shales	94	160	4.92	0.717657±27	0.69401	-143.3	28.7	5.12	0.108	0.512064 ±27	0.51183	-7.4
95-26	PSB	Black shales	69	188	7.94	0.706701±17	0.66889	-500.1	29.7	5.04	0.103	0.512069 ±52	0.51184	-7.0
Va.5	Visp.	Gabbroic core	235	3.31	0.04	0.705467±17	0.70527	16.6	13.4	4.11	0.186	0.513031 ±5	0.51262	8.2
Va.11	Visp.	Gabbroic core	178	23.9	0.39	0.706893±12	0.70503	13.2	14.5	4.06	0.169	0.512872 ±6	0.51250	5.7
Va.12	Visp.	Gabbroic core	168	12.6	0.22	0.706332±14	0.70529	16.9	10.5	3.58	0.206	0.513057 ±8	0.51260	7.8
Va.16	Visp.	Gabbroic core	135	4.72	0.10	0.706687±12	0.70620	29.8	11.8	3.98	0.203	0.513113 ±4	0.51266	9.0

Table 4: Rb-Sr and Sm-Nd analytical data of the tholeiitic suites from the Versoyen complex.

Rb, Sr, Nd and Sm concentrations were determined by ICPMS (refer to Table 2 and 3). (87Sr/86Sr)norm is normalized to 87Sr/86Sr = 8.3752, and (143Nd/144Nd) norm to 0.7219 [Wasserburg et al., 1981]. Analytical uncertainties are  $\pm 2\sigma$  for 87Sr/86Sr and 143Nd/144Nd, and are given in the table. Decay constant used are:  $\lambda$  (87Rb) = 0.0142 Ga-1 and  $\lambda$  (147Sm) = 0.00654 Ga-1. For the initial  $\epsilon_{Nd}$  calculation we used: (147Sm/144Nd)CHUR = 0.1967, and a present day value of (143Nd/144Nd)CHUR = 0.512638. For initial  $\epsilon_{Sr}$  we used: (87Rb/86Sr)UR = 0.0827, and a present day (87Sr/86Sr)UR = 0.7045.

Tableau 4: données des analyses Rb-Sr et Sm-Nd des tholeiites du complexe du Versoyen. Les concentrations en Rb, Sr, Nd et Sm concentrations sont déterminées sur une ICPMS (Se referer au Tableaux 2 et 3).



Fig. 1: Structural sketch and main units in the western Alps. Full line shows the location of Fig. 2 and 10 (PSB: Petit-Saint-Bernard pass; France-Italy).- External zone: 1- External crystalline massifs. - Internal zone: 2- Valaisan domain, 3- Undifferentiated Lower and Middle penninic nappes 4- "Schistes lustrés", 5- Ophiolitic suites, 6- Internal crystalline massifs. AA- Aar massif, DM- Dora Maira, MB- Mont-Blanc, La- Lanzo, Vo- Viso, Zs- Zermatt-Saas.

Fig. 1: Schéma structural et principales unités des Alpes occidentales. La localisation de la figure 2 et 10 est indiquée par un trait gras. (PSB: col du Petit-Saint-Bernard; frontière France Italie).- Zone Externe: 1- massifs cristallins externes. - zone Interne: 2- domaine Valaisan, 3- nappes penniques inférieures et moyennes (indifférenciées) 4- "Schistes lustrés", 5- cortège Ophiolitique, 6- massifs cristallins Internes. AA- Aar massif, DM- Dora Maira, MB- Mont-blanc, La- Lanzo, Vo- Viso, Zs- Zermatt-Saas.

Fig. 2: NW-SE geological cross sections through the PSB Versoyen complex (Location is shown in the Fig. 1). 1- External crystalline massifs, 2- Sedimentary cover of the External crystalline massifs, 3a- "Flysch de Tarentaise", 3b- Valaisan flysch, 4- Mesozoic and Pre-Mesozoic substratum of the Moutier unit, 5- Quartzite, 6a- Versoyen complex (mafic sills and sediments, 6b- Versoyen complex, (gneiss and ultramafic complex) 7- Calcareous slates of the Petit Saint Bernard unit, 8- Lower "zone Houillère" (lower penninic nappes), 9- Grand Saint Bernard nappe (Rutor). PF- Penninic Front, BF- Briançonnais Front.

Fig. 2: Coupe géologique NW-SE à travers le complexe du Versoyen (Localisation sur la Fig. 1). 1- massifs cristallins externes, 2- couverture sédimentaire des massifs cristallins externes, 3a- "Flysch de Tarentaise", 3b- flysch Valaisan, 4- substratum Mésozoïque et Pre Mésozoïque de l'unité de Moutier, 5- Quartzite, 6a- complexe du Versoyen (sills mafiques et sédiments, 6b- complexe du Versoyen (gneiss et complexe ultramafique) 7- Marno-calcaire de l'unité du Petit Saint Bernard, 8- "zone Houillère"inférieure (nappes penniques inférieures), 9- nappe du Grand Saint Bernard (Rutor). PF- Front Penninique, BF- Front Briançonnais.

Fig. 3: Restored lithostratigraphic sequences of the Versoyen complex near the Petit-Saint-Bernard pass (PSB) and Visp (Location are shown in the Fig. 1). The location and the name of the analyzed samples are listed in the left of the sequences.

Fig. 3: Séquence litho stratigraphique reconstituée du complexe du Versoyen près du col du Petit-Saint-Bernard (PSB) et de Visp (Localisation sur la Fig. 1). La localisation et le nom des échantillons analysés sont indiqués à gauche des séquences.

Fig. 4: (a) Phenocryst clinopyroxene composition of the Versoyen complex igneous rocks on a Ca-Mg-Fe pyroxenes diagram; (b) and (c) Discrimination diagrams [Leterrier et al., 1982], for clinopyroxene phenocrysts of the Versoyen complex igneous rocks.

Fig. 4: (a) Composition de phenocristaux de clinopyroxene de roches ignées du complexe du Versoyen dans un diagramme Ca-Mg-Fe des pyroxènes; (b) et (c) Diagrammes discriminants [Leterrier et al., 1982], pour les clinopyroxènes de roches ignées du complexe du Versoyen.

Fig. 5: Ti/Y versus Nb/Y tectonomagmatic discrimination diagram [Pearce, 1982] for the Versoyen complex igneous rocks.

Fig. 5: Diagramme discriminant du contexte tectonomagmatique basé sur Ti/Y versus Nb/Y [Pearce, 1982] pour les roches ignées du complexe du Versoyen.

Fig. 6: Chondrite-normalized REE patterns and primitive mantle-normalized spiderdiagrams [Sun and Mc Donough, 1989] for the Versoyen complex igneous and sedimentary rocks.

Fig. 6: Diagrammes REE normalisé au chondrite et "spiderdiagrams" [Sun et Mc Donough, 1989] pour les roches ignées et les sédiments du complexe du Versoyen.

Fig. 7: Ti/Y versus Zr/Y [Brewer et al., 1992] for the Versoyen complex igneous and sedimentary rocks.

Fig. 7: Diagramme discriminant du contexte tectonomagmatique basé sur Ti/Y versus Zr/Y [Brewer et al., 1992] pour les roches ignées du complexe du Versoyen.

Fig. 8:  $\epsilon_{Nd}(337\text{Ma})$  and  $\epsilon_{Sr}(T=337\text{Ma})$  plot for the Versoyen complex igneous and sedimentary rocks.

Fig. 8: Diagramme  $\epsilon_{Nd}(337\text{Ma})$  versus  $\epsilon_{Sr}(T=337\text{Ma})$  pour les roches ignées et les sédiments du complexe du Versoyen.

Fig. 9:  $\epsilon_{Nd}(337\text{Ma})$  versus Sm/Nd and Zr/Ti for the Versoyen complex. Same symbols as Fig. 8 for the basaltic dikelet, sill cores, clinopyroxenes, sill margins and felsic rocks

Fig. 9: Diagrammes  $\epsilon_{Nd}(337\text{Ma})$  versus Sm/Nd et Zr/Ti pour les roches ignées du complexe du Versoyen. Même symboles que sur la figure 8 pour les petits dykes basaltiques, la partie centrale des sills, les clinopyroxènes, les épontes des sills et les roches feldspathiques.

Fig. 10: an interpretation of the deep seismic ECORS seismic line based on a coherency-weighted-migration procedure of the seismic sections [Mugnier and Marthelot, 1991] (Vertical scale in s. TWT).

Fig. 10: Une interprétation du profil sismique grande profondeur ECORS, basée sur une migration automatique avec pondération sur la cohérence du signal [Mugnier et Marthelot, 1991] (Echelle verticale en secondes- temps-double).

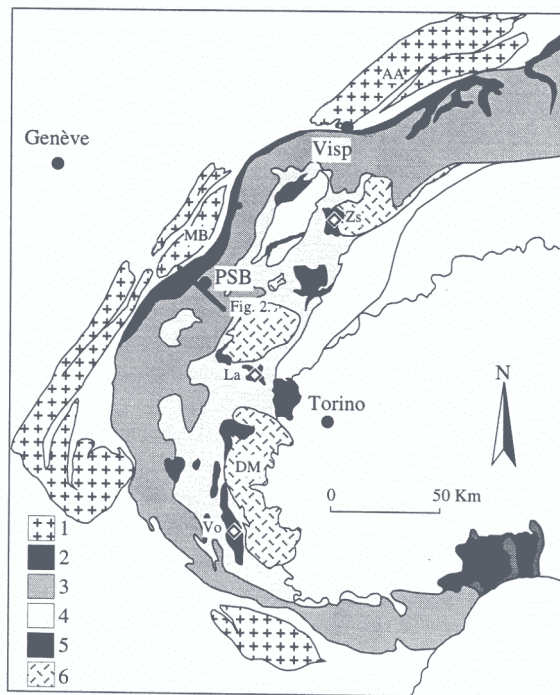


Fig. 1

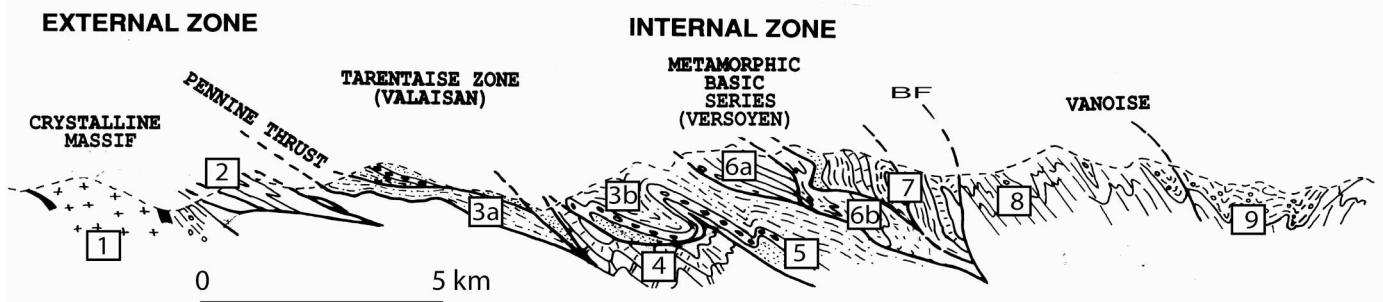


Fig. 2

## Versoyen complex

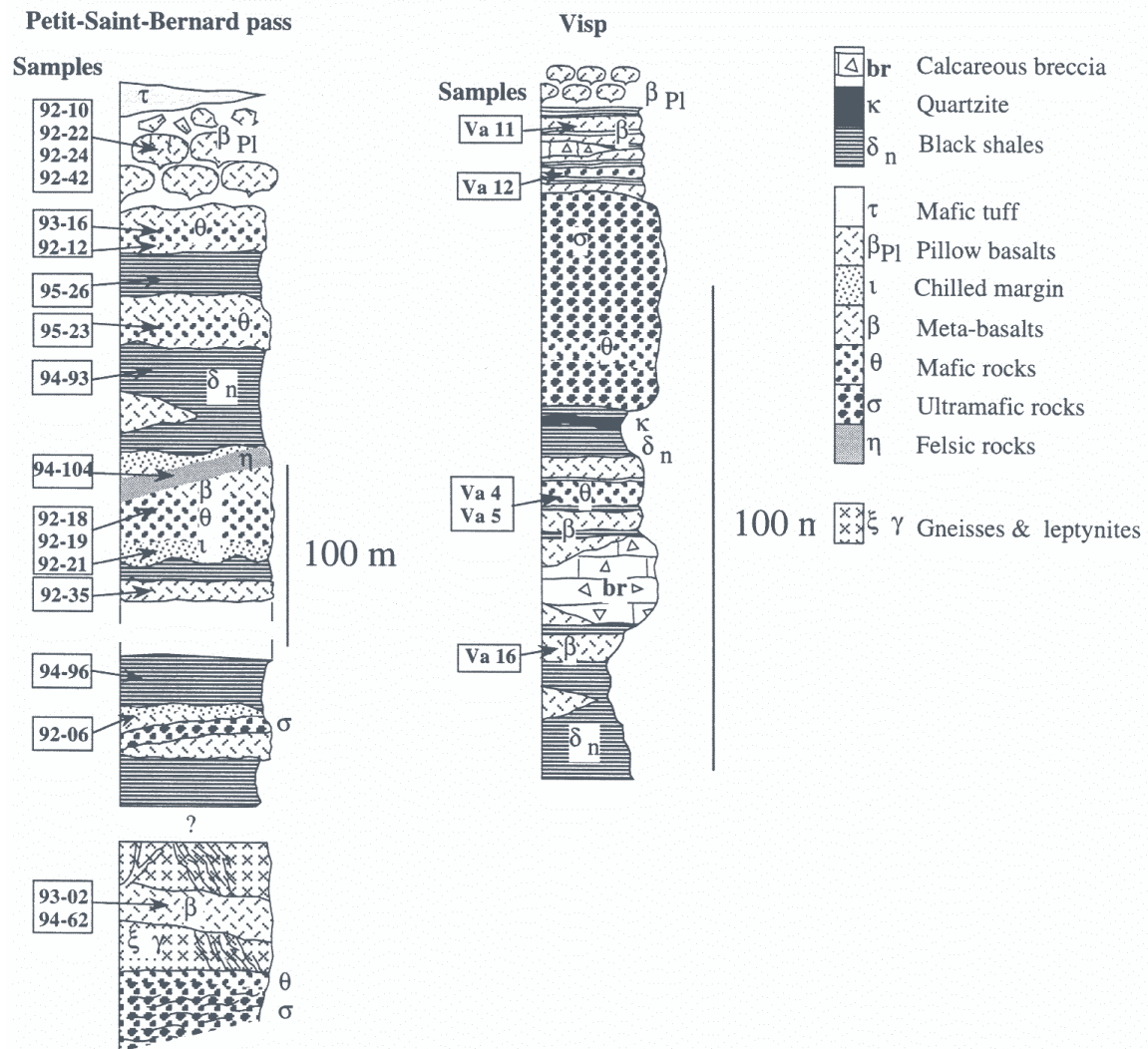


Fig. 3

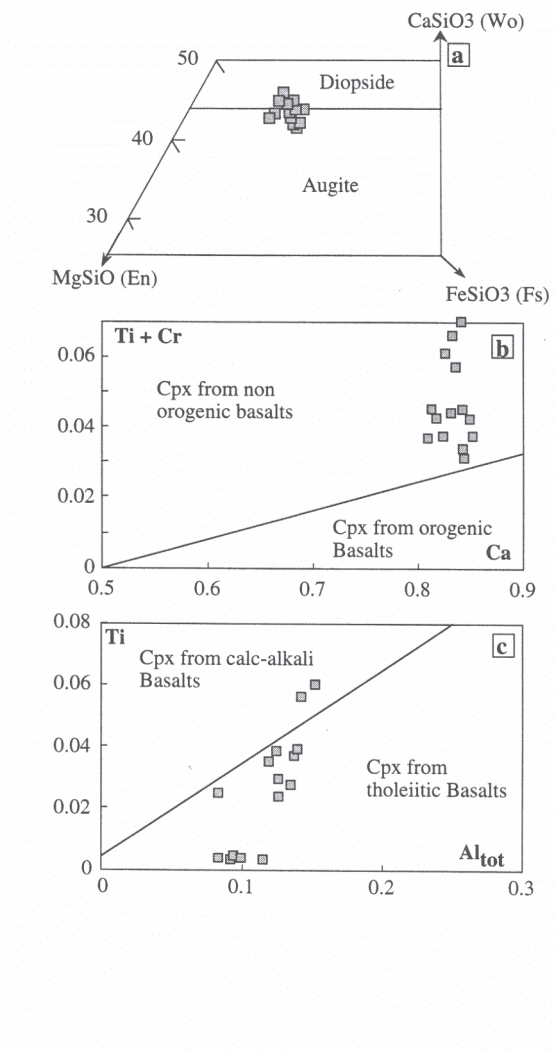


Fig. 4

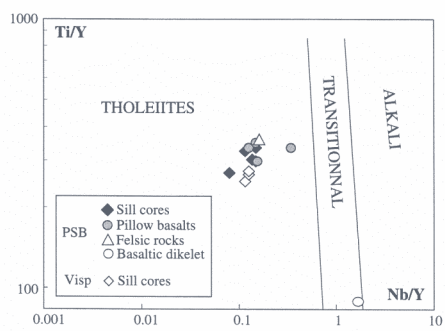
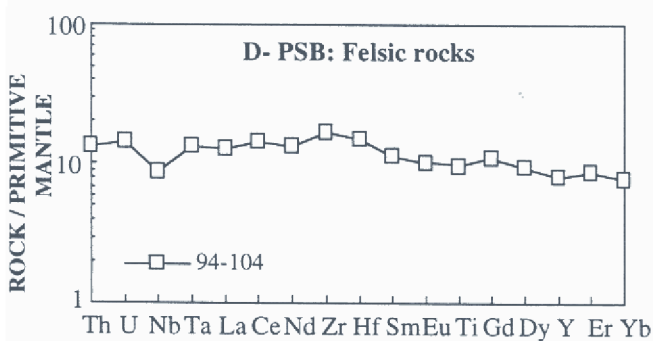
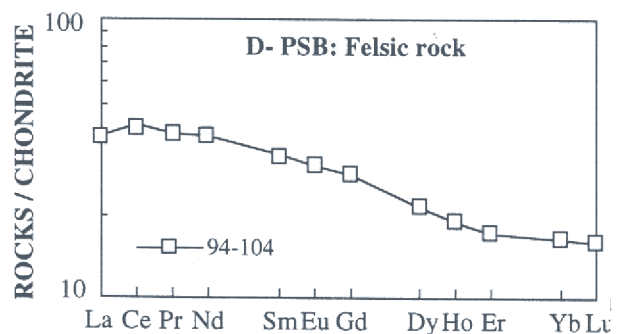
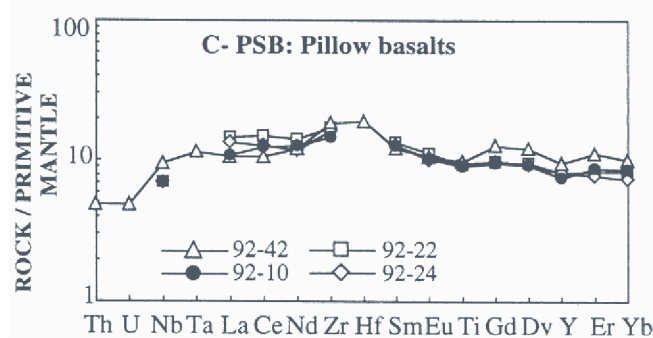
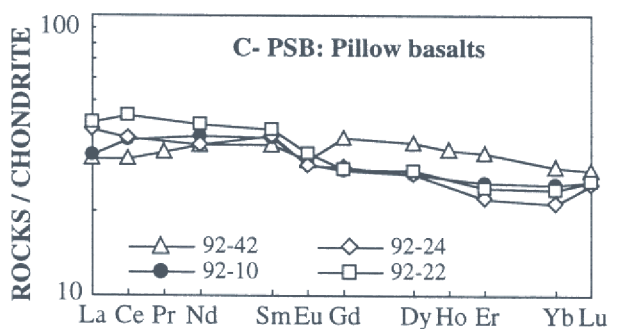
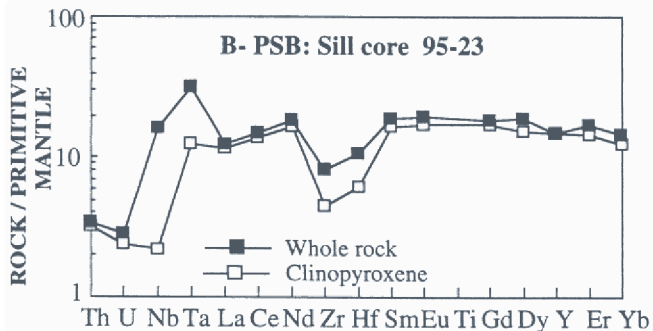
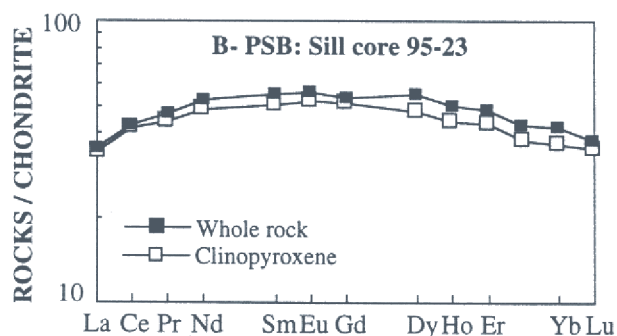
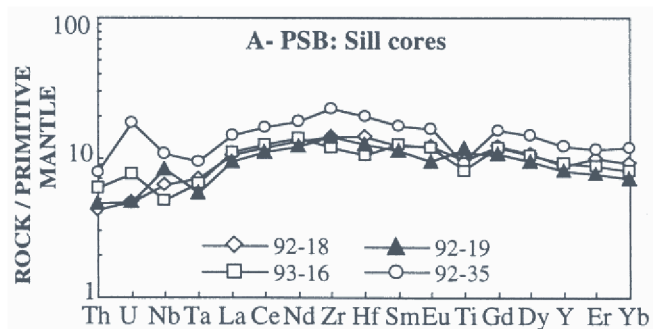
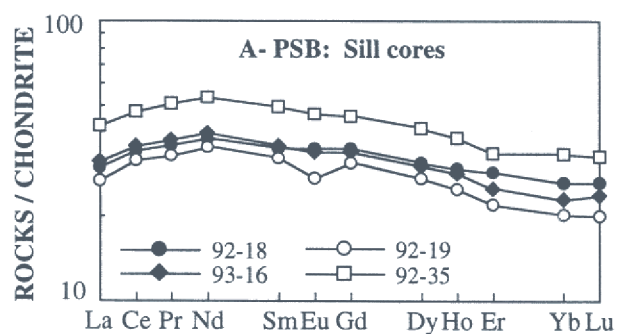


Fig. 5



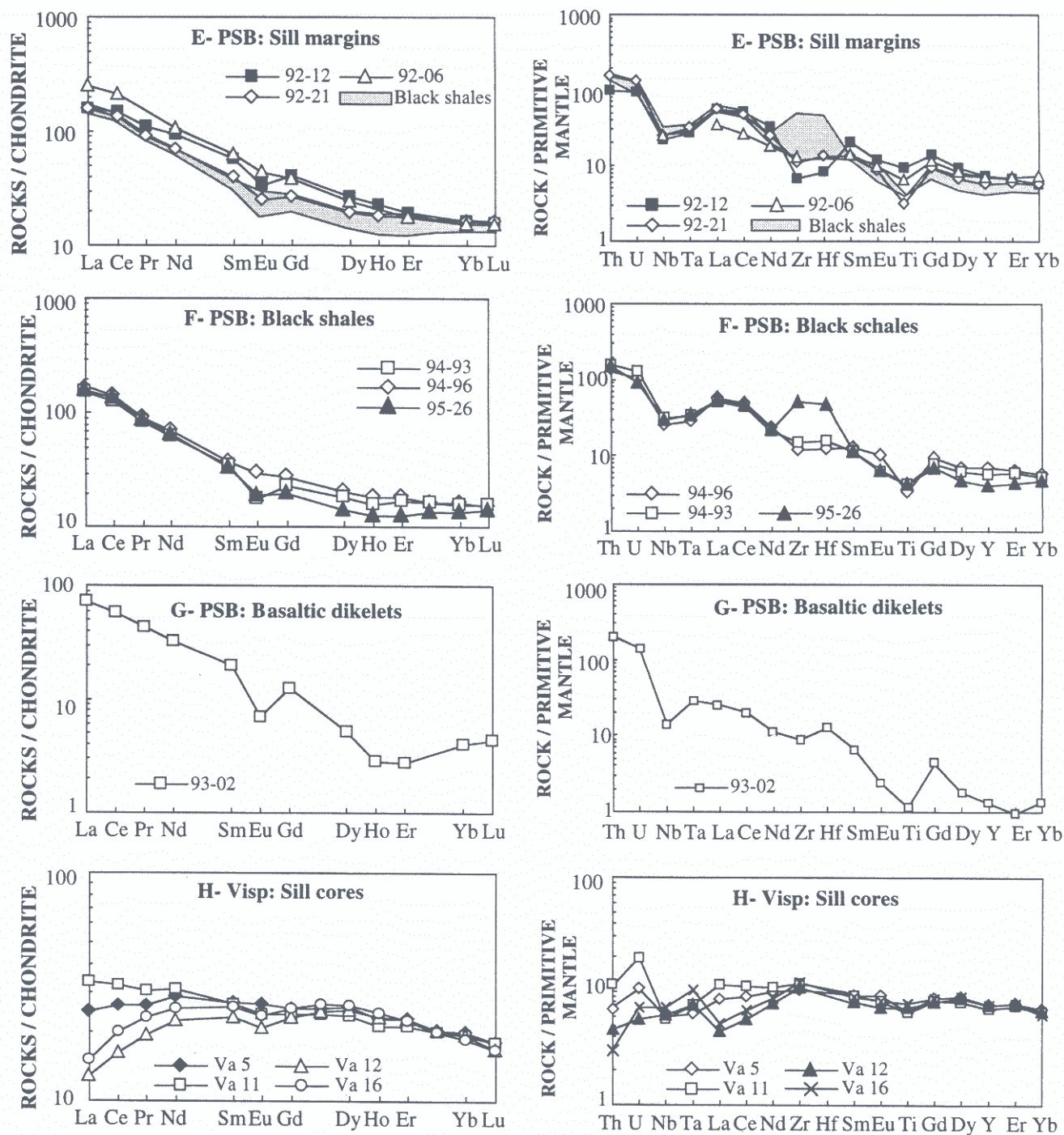


Fig. 6



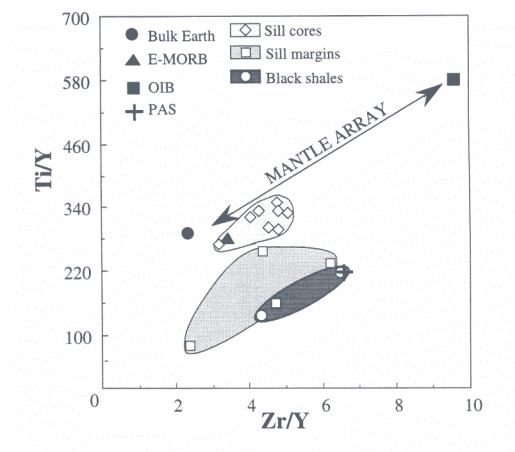


Fig. 7

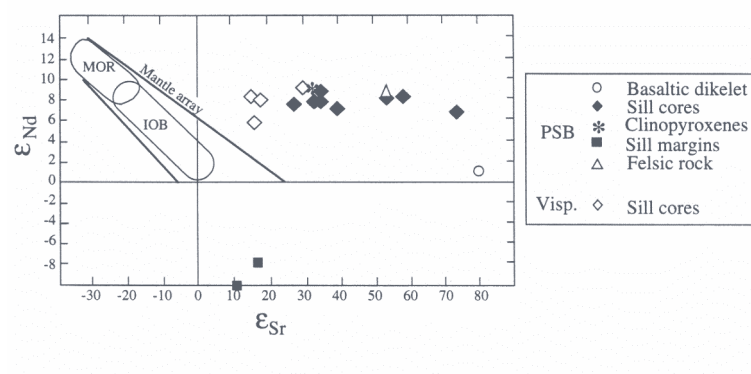


Fig. 8

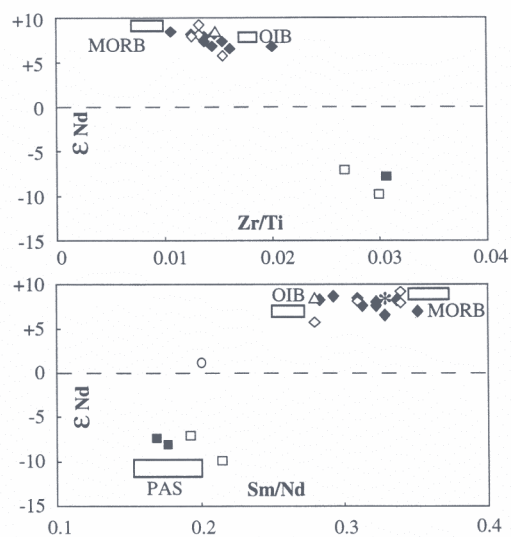


Fig. 9

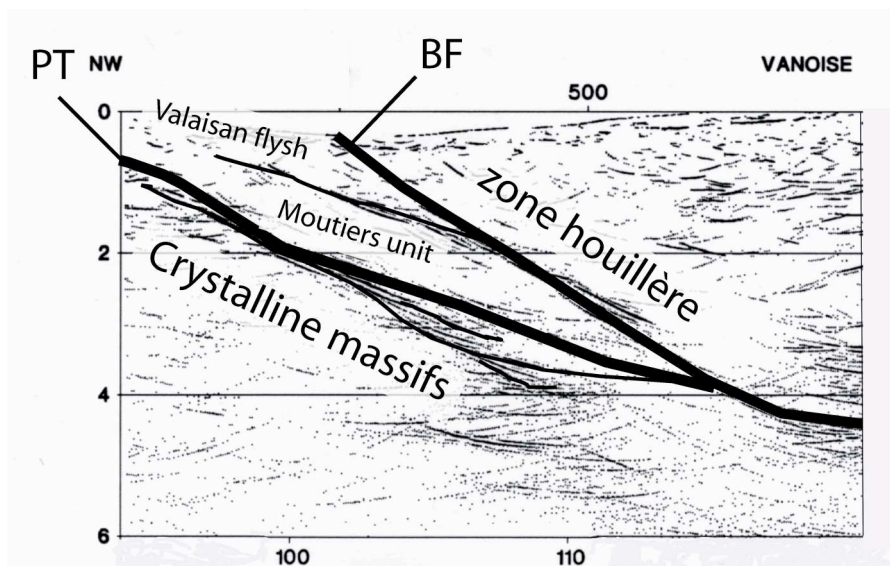


Fig. 10